MODELLING AND SIMULATION OF A WHEELED LAND VEHICLE

A THESIS SUBMITTED TO
THE GRADUATE SCHOOL OF NATURAL AND APPLIED SCIENCES
OF
MIDDLE EAST TECHNICAL UNIVERSITY

BY

ALP LAFCI

IN PARTIAL FULFILLMENT OF THE REQUIREMENTS
FOR
THE DEGREE OF MASTER OF SCIENCE
IN
ELECTRICAL AND ELECTRONICS ENGINEERING

JANUARY 2010

Approval of the thesis:

MODELLING AND SIMULATION OF A WHEELED LAND VEHICLE

Submitted by **ALP LAFCI** in partial fulfillment of the requirements for the degree of **Master of Science in Electrical and Electronics Engineering Department, Middle East Technical University** by,

Prof. Dr. Canan Özgen _____
Dean, Graduate School of **Natural and Applied Sciences**

Prof. Dr. İsmet Erkmen _____
Head of Department, **Electrical and Electronics Engineering**

Prof. Dr. Kemal Leblebicioğlu _____
Supervisor, **Electrical and Electronics Engineering Dept., METU**

Examining Committee Members:

Prof. Dr. Mustafa Kuzuoğlu _____
Electrical and Electronics Engineering Dept., METU

Prof. Dr. Kemal Leblebicioğlu _____
Electrical and Electronics Engineering Dept., METU

Prof. Dr. Y. Samim Ünlüsoy _____
Mechanical Engineering Dept., METU

Prof. Dr. İsmet Erkmen _____
Electrical and Electronics Engineering Dept., METU

Assoc. Prof. Dr. Tolga Çiloğlu _____
Electrical and Electronics Engineering Dept., METU

Date: 15.12.2009

I hereby declare that all information in this document has been obtained and presented in accordance with academic rules and ethical conduct. I also declare that, as required by these rules and conduct, I have fully cited and referenced all material and results that are not original to this work.

Name, Last name: Alp Lafcı

Signature :

ABSTRACT

MODELLING AND SIMULATION OF A WHEELED LAND VEHICLE

Lafcı, Alp
M.S., Department of Electrical and Electronics Engineering
Supervisor: Prof. Dr. Kemal Leblebicioğlu

January 2010, 66 Pages

Land transportation is the main form of transportation around the world. Since the invention of the car land transportation changed drastically. As the cars took a solid part in human lives with the developments in electronics and robotics unmanned land vehicles are the future of both commercial and military land transportation. Today armies want unmanned land vehicles to provide logistical support to the units near threat zones and commercial firms want them to deliver goods more reliably and with less expense.

In this thesis, mainly, a 6DoF dynamical model for a four wheeled land vehicle is developed and an autopilot design is presented using PID techniques. For dynamical modeling of the vehicle internal combustion engines, transmissions, tires, suspensions, aero dynamical drag forces and brakes are studied and the model is tested over some scenarios for evaluating its performance.

Keywords: Unmanned Land Vehicle, Autopilot, Car, PID, Optimal Control.

ÖZ

TEKERLEKLİ KARA TAŞITININ MODELLENMESİ VE SİMULASYONU

Lafcı, Alp
Yüksek Lisans., Elektrik ve Elektronik Mühendisliği Bölümü
Tez Yöneticisi: Prof. Dr. Kemal Leblebicioğlu

Ocak 2010, 66 Sayfa

Kara ulaşımı dünyanın en genel ulaşımı şeklidir. Arabaların icadından itibaren kara ulaşımı son derece değişmiştir. Arabalar insan hayatından ayrılamaz bir rol üstlendikçe ve elektronik ve robotik alanlarındaki gelişmelerle beraber insansız kara taşıtları askeri ve sivil kara ulaşımının geleceğini temsil etmektedir. Günümüzde ordular düşman hatlarının yakınına lojistik destek sağlamak için insansız kara taşıtlarını tercih ederken sivil kuruluşlar daha etkin ve ucuz taşımacılık için insansız kara araçlarını istemektedirler.

Bu tez çalışmasında temel olarak dört tekerlekli bir kara aracının 6 özgürlük dereceli dinamik modeli ve PID kontrolcülerle çalışacak bir otopilot tasarımı sunulmuştur. Dinamik modelleme için içten yanmalı motorlar, güç aktarım sistemleri, lastikler, süspansiyonlar, aerodinamik sürüklenme kuvvetleri ve frenler üzerine incelemeler yapılmış ve oluşturulan model çeşitli senaryolarla doğrulanması için test edilmiştir.

Anahtar Kelimeler: İnsansız Kara Aracı, Otopilot, Araba, PID, Optimal Kontrol.

Hayatı benim için değerli kılan tüm sevdiklerime…

ACKNOWLEDGMENTS

I would like to express my appreciation to my supervisor Prof. Dr. Kemal LEBLEBİCİOĞLU for his guidance, support and suggestions throughout the research.

I would like to acknowledge the manager of Thermal Systems Design Department in ASELSAN INC, Mr. Alper ÜNSOY and all of my colleagues for their support especially Mr. Ali Erdem ÖZCAN.

Last, but definitely not the least, I would like to thank to my family, Mr. Ali LAFCI, Mrs. Reyhan LAFCI and my brother Mr. Oğuz LAFCI for their motivation and support to me in order to complete thesis. I also want to thank my girlfriend, Seda ŞAYİN; for her endless patience and sympathy she showed to me during my graduate school attendance.

TABLE OF CONTENTS

LIST OF TABLES

TABLES:

LIST OF FIGURES

FIGURES:

LIST OF SYMBOLS

F_X	Force in body longitudinal axis
F_Y	Force in body lateral axis
F_Z	Force in body vertical axis
F^E	Normal-Earth fixed frame
F^B	Body frame
x_E, y_E, z_E	Normal-Earth fixed frame axes
x_b, y_b, z_b	Body frame axes
ψ	Yaw angle
θ	Pitch angle
Φ	Roll angle
T_{EB}	Transformation matrix that represents a transformation from F^E to F^B
T_ψ	Yaw transition
T_θ	Pitch transition
T_ϕ	Roll transition
CG	Center of gravity of the vehicle
n_{Pmax}	Maximum power output speed
T_{max}	Maximum torque output
P_{max}	Maximum power output
T_{ENGINE}	Engine torque
u, v, w	Components of vehicle velocity vector in body frame
η_{oveall}	Overall efficiency of the internal combustion engine
T_{NET}	Net torque output
$T_{AIRDRAG}$	Air drag load on engine
T_{trans}	Transmission torque
T_{eng}	Engine torque that goes to transmission
n_i	Current gear ratio i

W_{trans}	Rotational speed of transmission
W_{eng}	Rotational speed of engine
v_{bX}	Body x-axis velocity
v_{bY}	Body y-axis velocity
$\mu_{rolling}$	Rolling friction coefficient
μ_{trans}	Translational friction coefficient
$F_{y\delta}$	Lateral force due to cornering stiffness
C_{α}	Cornering stiffness coefficient
δ	Sideslip angle
$F_{Yw\_to\_Yb}$	Lateral cornering force projected to body y-axis
$F_{Yw\_to\_Xb}$	Lateral cornering force projected to body x-axis
FXi	Longitudinal force on body frame produced by tire# i, i: 1, 2, 3, 4
FYi	Lateral force on body frame produced by tire# i, i: 1, 2, 3, 4
Fxti	Longitudinal force produced by tire# i, i: 1, 2, 3, 4
Fyti	Lateral force produced by tire# i, i: 1, 2, 3, 4
δ_i	Sideslip angle of tire# i, i: 1, 2, 3, 4
Fz_front	Front vertical suspension force
Fz_rear	Rear vertical suspension force
K	Suspension spring constant
C	Suspension damping constant
a	Longitudinal distance of front tires to CG
b	Longitudinal distance of rear tires to CG
c	Lateral distance of tires to CG
Fbrake	Brake force
M	Mass of the vehicle
g	Gravity
Fy_forward	Front tires lateral slip force
Fy_rear	Rear tires lateral slip force
l_f	Distance of the front tires to CG
l_r	Distance of the rear tires to CG
A	Contact area that is affected from drag

C_d	Aerodynamic friction coefficient
F_D	Air drag force
ρ	Air density
v	Velocity in the axis of air drag force
F_{Xi}	Longitudinal force on tire i, i: 1, 2, 3, 4
F_{Yi}	Lateral force on tire i, i: 1, 2, 3, 4
F_{Zi}	Vertical force on tire i, i: 1, 2, 3, 4
Jx, Jy, Jz	Inertias around body axes
ωx, ωy, ωz	Rotational speeds around body axes
K_P	Proportional constant of PID controller
K_I	Integral constant of PID controller
K_D	Derivative constant of PID controller
β	Brake pedal angle

CHAPTER 1

INTRODUCTION

1.1 Motivation and Contribution

The motivation of this thesis work is to create a 6DoF dynamic wheeled vehicle model in order to design an optimal controller for the modeled system in order to provide autonomous wheeled land transportation.

The designed optimal controller would provide a minimum cost track follower for the modeled system. The resultant outputs will be employed for the modeled system in order to make it to follow a desired track without any user interference.

1.2 General Information

Land transportation has been changed dramatically after the introduction of internal combustion engines and hence the automobiles. Beginning from its first appearance on streets, cars begin to change and evolve reflecting current trends in fashion, use, performance, etc. Cars reduced transportation time and increased traveled distances [1]. Although cars are on the roads for more than a century most of the basic systems that a car depends for land locomotion are still the same.

From the dynamical aspect a car needs the following items to operate [2]:

- An internal combustion engine,
- A power train,
- A steering mechanism,
- Suspensions,
- Tires,
- Brakes.

When the mentioned items are connected, a dynamic system is obtained. The car system has the following inputs:

- Steering Angle Input,
- Throttle Input,
- Brake Input.

A basic system diagram of a car is given in Figure 1 below:

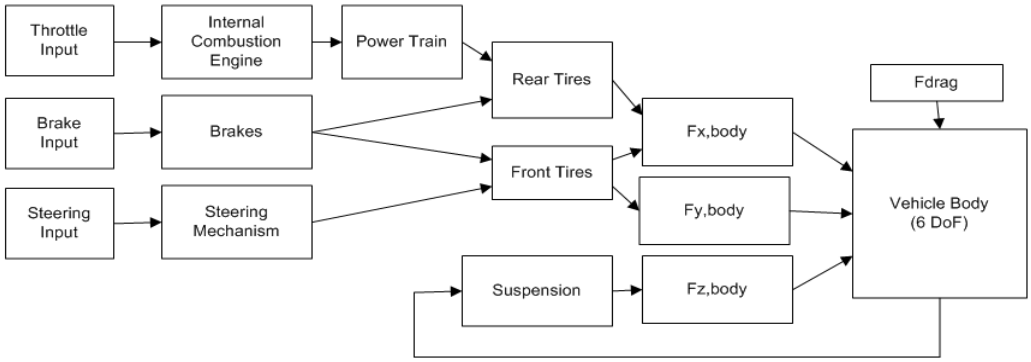

Figure 1 System Diagram of a Car

The driver gives inputs via pedals and steering wheel. Pedals change the vertical force acting by increasing or decreasing the longitudinal force acting on the vehicle [2]. The steering wheel changes the yaw angle of the vehicle by applying lateral force on the vehicle [3].

The throttle pedal excites the internal combustion engine to produce torque. The produced torque therefore goes through the power train to be increased and transferred to the rear tires. Due to friction the rear tires converts this given torque to a linear force (F_x) along the body longitudinal axis.

The brakes pedal activates the braking system to convert kinetic energy to heat energy by applying friction force on the wheels; hence acting as a negative linear force along the body longitudinal axis (F_x).

The steering wheel sets the angle of the front wheels and hence produces both a lateral force (F_y) and a breaking effect (F_x).

The last force generating sources are the suspensions and the drag force. They are both out of driver's control. The suspensions generate forces in the vertical direction to the vehicle body (F_z) with respect to its former position to attenuate the road noises and sharp maneuvers. The drag force is acting on both body longitudinal and lateral axes and is related with vehicle chassis design and current vehicle speed in the mentioned body axes.

1.3 Outline of the Thesis

The thesis is organized in the following manner:

In Chapter 2, the forces acting on the 6 Degrees of Freedom model of the car are modeled. The forces are grouped in two divisions, namely the planar and vertical forces and for each force group the subsystems of the car are also modeled.

In Chapter 3, a non-linear 6 Degrees of Freedom model of the car is constructed depending of the forces modeled in Chapter 2 and the drag forces acting on the vehicle body which are modeled in this chapter. Also the constructed Simulink model is given here.

In Chapter 4, two PID (proportional integral derivative) controllers and an autopilot is constructed in order to test the given 6DoF Simulink car model. The section also contains the simulation results of the complete model for test settings.

In Chapter 5, an optimal controller is designed for the system and a simulation is performed.

In Chapter 6, results of simulations are concluded and recommendations for future works are presented.

CHAPTER 2

MODELLING OF FORCES

In order to obtain a convenient 6 DoF dynamic model of a car, it is an obligation to decide how to model the car by choosing complexity of the model and its parts and what will be performed with the constructed model. One approach for constructing a 6 DoF model is thinking the car as a spring-mass system under the influence of tire forces [2].

However since a car is a complex nonlinear system some assumptions must be made to simplify the system without losing the accuracy considerably. These assumptions are listed below:

1. The car is a lumped point mass and that it is situated point at the center of gravity,
2. The vehicle moves in a horizontal plane and all of the tires touch ground at all times,
3. Aerodynamic drag is included in the model but only in translational motion
4. Tire inertias are not included in the system,
5. Tires only apply planar forces to the vehicle body frame on X-Y plane,
6. Suspensions only apply vertical forces to the vehicle body frame along Z axis,
7. The road surface conditions are the same with no road input,
8. The small angle approximations will be applied,
9. The tires are assumed to have side slip and negligible longitudinal slip,
10. The transmission is automatic such that there is no clutch,
11. Tires have a camber angle of zero at all times,
12. During steering both of the front wheels steering angles are same.

In order to sum these assumptions a drawing is given below (Figure 2). The above assumptions imply that the tires are treated as force generators on the planar axis and can be treated as junction points after the force they generate is calculated [5]. The vehicle chassis body angles are calculated from suspension forces and planar forces inputs. However suspensions do not change the planar motion and suspension forces are in parallel to the vehicle vertical axis at all times. Hence the resultant model is a 6DoF one but is run on a plane.

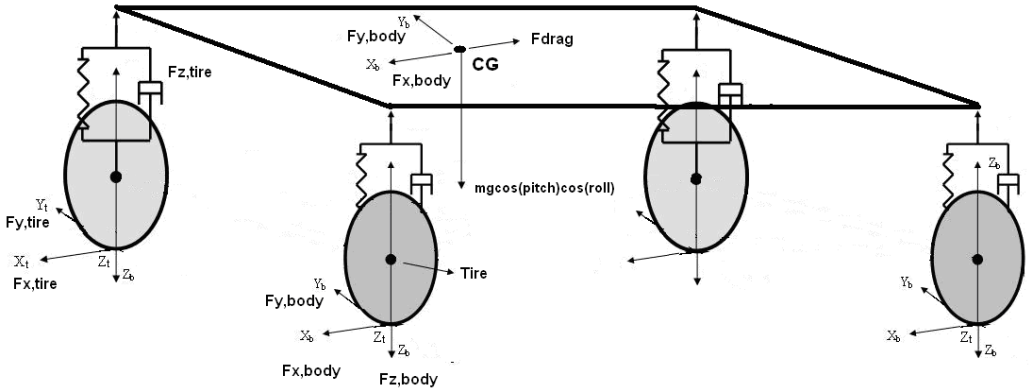

Figure 2 Drawing Considering the Above Assumptions

The model that will be constructed during this thesis work will be used for designing an autopilot to navigate a car. Considering this the model complexity seems to be enough since it focuses on the center of gravity of the vehicle so that the final point of the motion can be found by integrating the initial velocity of the vehicle and adding a given initial point.

In order to obtain the 6 DoF model, it is needed to find the tire, suspension and drag forces. After they must be projected to body coordinates such that the net force that affects the center of gravity could be found.

In order to correctly calculate these projections first the definitions of the reference frames must be given to calculate the net forces on the car center of gravity.

2.1 Reference Frames

Two coordinate frames must be defined in order to describe the motion of the vehicle.

1. Normal Earth-fixed frame F^E,
2. Body frame F^B.

Both of them are three-dimensional, orthogonal and right-handed [6].

2.1.1 Normal Earth-Fixed Frame

The origin of the frame is the fixed point O on the Earth center. The axes are x_E,y_E,z_E.

1. The x-axis is directed towards the geographical North,
2. The z-axis is directed towards the descending direction of gravitational attraction and,
3. The y-axis is the complementing axis.

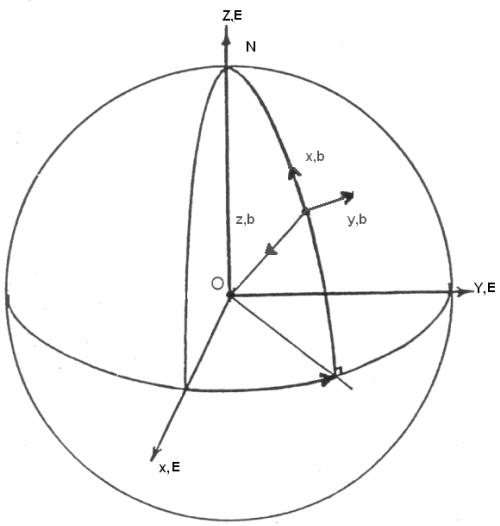

Figure 3 Normal Earth-Fixed Coordinate System

2.1.2 Body Frame

The body frame of a car is standard and named as Vehicle Body Coordinate System. The origin of the body frame is related to the vehicle body and the center of gravity. The body frame axes are x_b,y_b,z_b. The x-axis (roll axis), points towards the front of the vehicle, the y-axis (pitch axis), is directed towards the lateral side of the vehicle, and the z-axis (yaw axis), is the complementing axis. CG point is the center of mass.

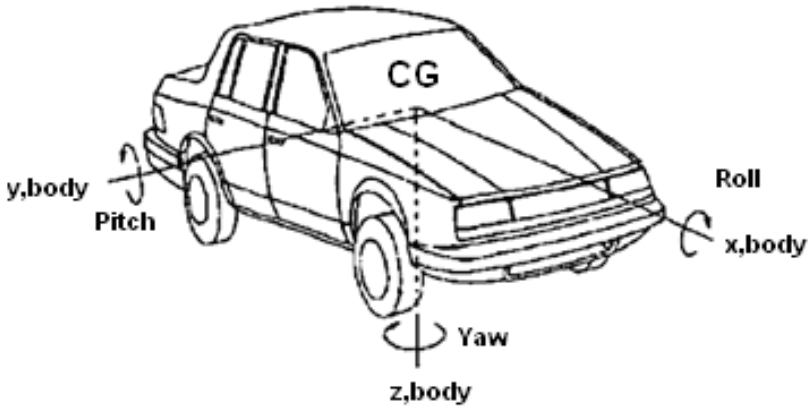

Figure 4 Vehicle Body Coordinate System (w.r.t. SAE convention) [2]

2.1.3 Transformations between the Reference Frames

After two frames have been established, it is useful to define their relations by means of angles. There are three angles in each coordinate system, which allow the transformation from the Normal Earth Fixed Frame (F^E) to the Body Frame (F^B) [6].

1st rotation	ψ yaw angle	about axis z_E
2nd rotation	θ pitch angle	about axis y_E
3rd rotation	Φ roll angle	about axis x_E

Yaw, pitch and roll angles are called Euler angles. These three transformations are associated with the formulations below:

$$F^E = (T_\psi T_\theta T_\phi) \cdot F^B = T_{EB} \cdot F^B \tag{2.1}$$

$$T_\varphi = \begin{pmatrix} \cos\psi & -\sin\psi & 0 \\ \sin\psi & \cos\psi & 0 \\ 0 & 0 & 1 \end{pmatrix},\ T_\theta = \begin{pmatrix} \cos\theta & 0 & \sin\theta \\ 0 & 1 & 0 \\ -\sin\theta & 0 & \cos\theta \end{pmatrix},\ T_\phi = \begin{pmatrix} 1 & 0 & 0 \\ 0 & \cos\Phi & -\sin\Phi \\ 0 & \sin\Phi & \cos\Phi \end{pmatrix}$$

$$T_{EB} = \begin{pmatrix} \cos\psi & -\sin\psi & 0 \\ \sin\psi & \cos\psi & 0 \\ 0 & 0 & 1 \end{pmatrix} \cdot \begin{pmatrix} \cos\theta & 0 & \sin\theta \\ 0 & 1 & 0 \\ -\sin\theta & 0 & \cos\theta \end{pmatrix} \cdot \begin{pmatrix} 1 & 0 & 0 \\ 0 & \cos\Phi & -\sin\Phi \\ 0 & \sin\Phi & \cos\Phi \end{pmatrix}$$

$$= \begin{pmatrix} \cos\theta\cos\psi & \sin\theta\sin\Phi\cos\psi - \sin\psi\cos\Phi & \cos\psi\sin\theta\cos\Phi + \sin\Phi\sin\psi \\ \sin\psi\cos\theta & \sin\theta\sin\Phi\sin\psi + \cos\psi\cos\Phi & \sin\theta\cos\Phi\sin\psi - \sin\Phi\cos\psi \\ -\sin\theta & \cos\theta\sin\Phi & \cos\theta\cos\Phi \end{pmatrix} \tag{2.2}$$

T_{EB} representation describes the transformation from the Normal Earth Fixed Frame to the Body Frame.

However as the vehicles motion is assumed to be planar the final reference system looks like as in the figure below.

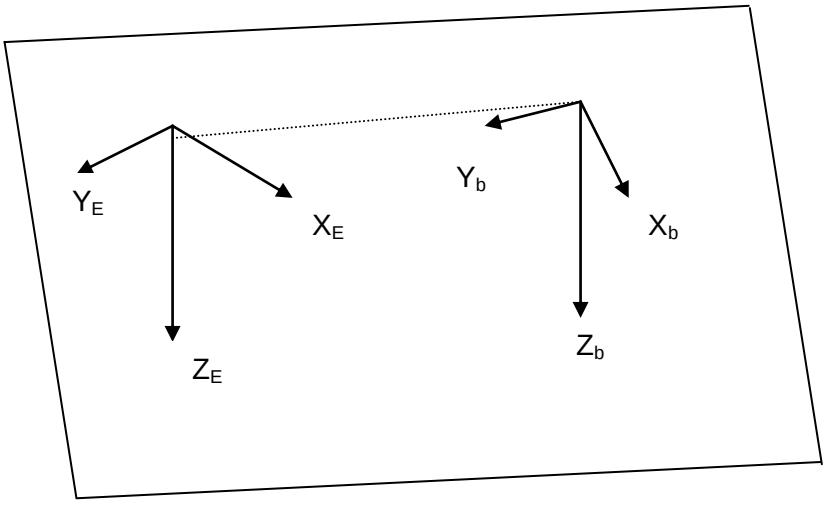

Figure 5 Concluded Reference System

2.2 Force Modeling

As mentioned at the introduction part a car has force generating parts that allow it to perform and control movement. In order to model a car these force generating parts must be dynamically modeled.

In this chapter the following car subsystems will be modeled:

1. Internal combustion engine and transmission,
2. Tires,
3. Steering mechanism,
4. Suspensions,
5. Brakes,
6. Slip,
7. Drag.

2.2.1 Internal Combustion Engine

The internal combustion engine is the power provider for the car. The basic duty of the engine is to convert the chemical energy in the fuel to the kinetic energy [4]. Since the motor is the most complex and nonlinear part of a car it is required to be simplified at a reasonable level.

Engines have two major outputs which are the engine power and the engine torque. So engines are provided with their power-torque graphs. However internal combustion engines differ from electric engines for both of these two outputs.

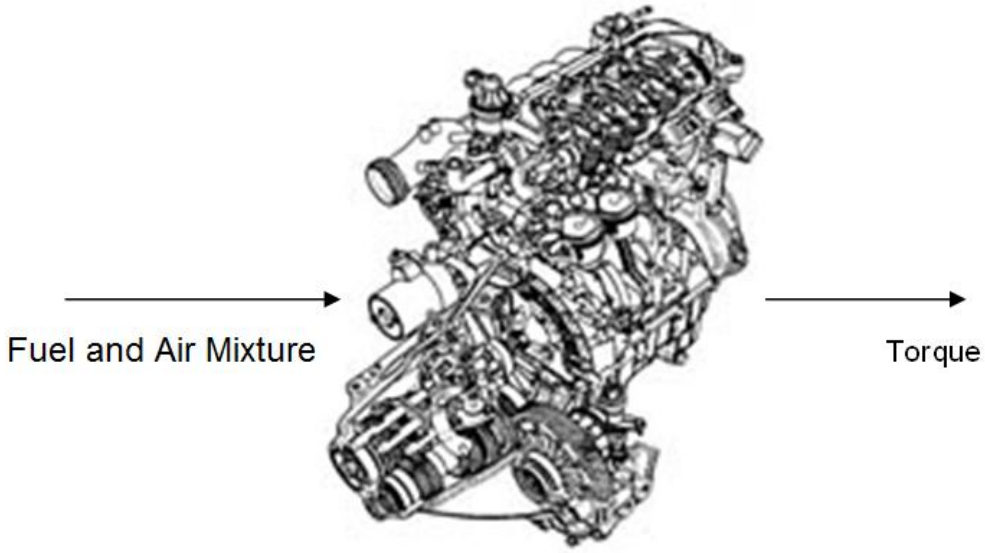

Figure 6 Internal Combustion Engine

For dc electric motors the torque starts from a maximum value as the engine runs faster. This causes a declining torque line and a parabolic power curve [7]. So for a high torque application without a gearbox the engine must be run at low speed values. For the high power applications n_{Pmax} must not be overridden because engine speeds higher then n_{Pmax} are less efficient except the situations where high speed values must be obtained without a gearbox attached to the engine.

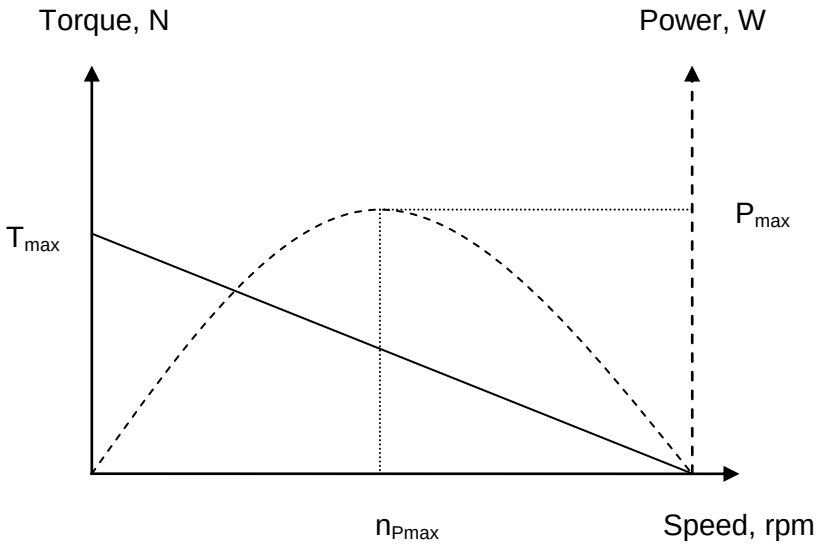

Figure 7 Torque-Power Graph of a DC Motor [7]

However for internal combustion engines the torque-power graph is different. Such a graph for a general car engine is shown below:

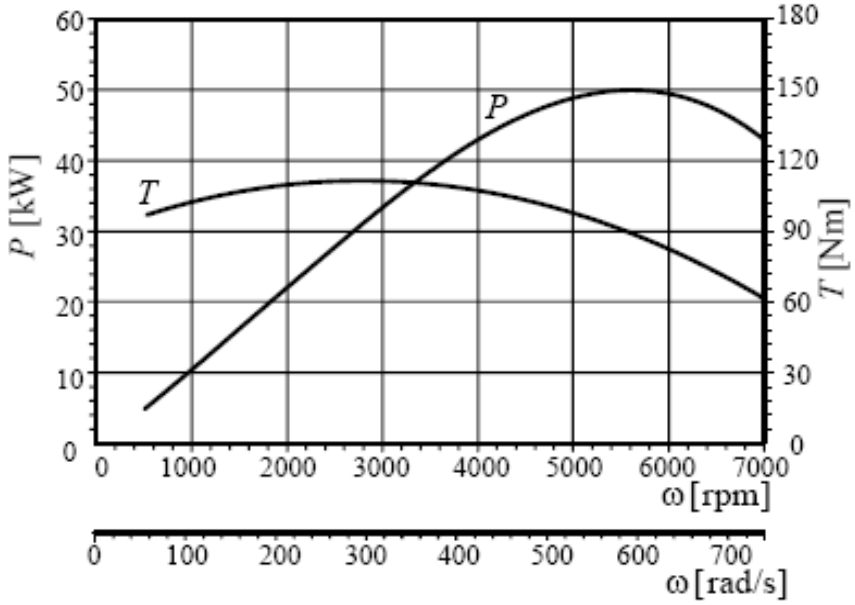

Figure 8: Power-Torque Plot of a Gasoline Engine [5]

As seen from the figure the torque reaches its peak value faster than the power of the engine. However after a peak value it starts to decrease whereas power still increases as with the rising engine speed. Inevitably power soon reaches its peak value at some engine speed and starts to decrease as with the torque as the engine runs faster [5].

In order to simulate an internal combustion engine four different approaches can be made:

1. Modeling the engine from its thermodynamic equations [4],
2. Modeling the engine as function that gives us torque-power values for a given engine speed [5],
3. Modeling the engine as a black box which takes an energy input and produces an output with respect to given engine states [8],

4. Modeling the engine with respect to a given Torque-Throttle Angle plot for various engine speeds.

Among these given modeling options the fourth one is chosen due to its capability of approximating the engine behavior at various control inputs at different engine speed values. Once the plot is converted to a data table that includes torque, throttle angle and engine speed, it is now possible to interpolate the torque value for a given throttle input for any engine speed.

Torque-throttle angle plot is shown below:

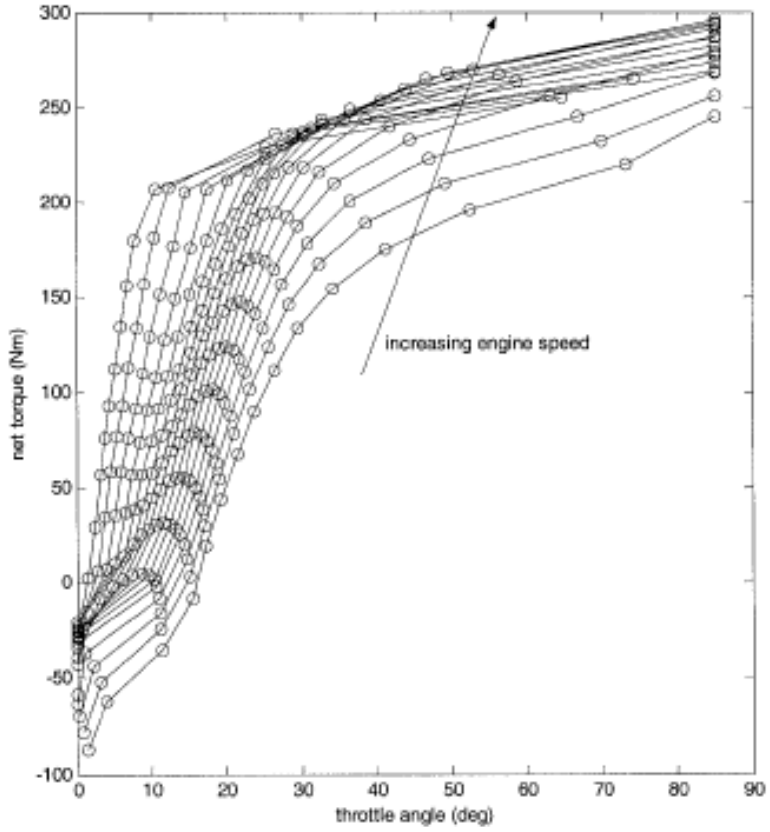

Figure 9 Torque-Throttle Angle Plot for Various Engine Speeds [28]

Another version of this plot is torque vs. engine speed version which gives a better understanding of the effect of throttle input at the engine torque output (Figure 10)

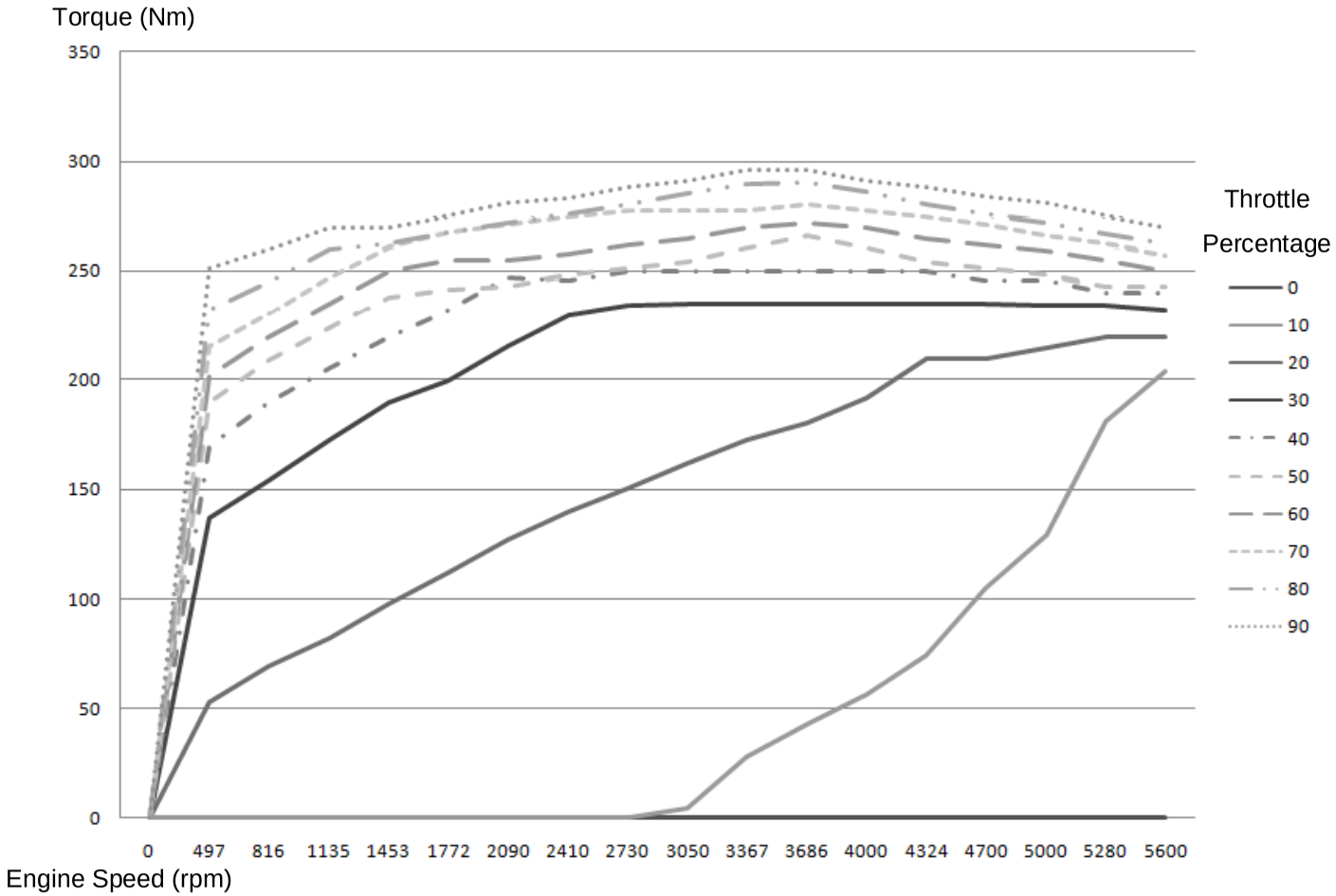

Figure 10 Torque vs. Engine Speed with Respect to The Throttle Percentage

Engine speeds that the plot is based on are given in the table below:

Table 1 Torque Output for Respective Engine Speed and Throttle Angle

Engine Speed(rpm)	Throttle Angle (α)									
	0	10	20	30	40	50	60	70	80	90
0	0	0	0	0	0	0	0	0	0	0
497	0	0	53	137	170	190	202	215	232	252
816	0	0	69	154	190	209	220	230	245	260
1135	0	0	82	173	206	224	235	247	260	270
1453	0	0	98	190	220	238	250	261	263	270
1772	0	0	112	200	232	242	255	267	268	275
2090	0	0	127	216	247	243	255	271	272	281
2410	0	0	140	230	246	248	258	274	276	283
2730	0	0	151	234	250	251	262	277	280	288
3050	0	4	162	235	250	254	265	277	285	291
3367	0	28	173	235	250	260	270	277	289	296
3686	0	43	181	235	250	266	272	280	290	296
4000	0	56	192	235	250	260	270	277	286	291
4324	0	74	210	235	250	254	265	274	280	288
4700	0	105	210	235	246	251	262	271	276	284
5000	0	129	215	234	246	248	259	266	272	281
5280	0	181	220	234	240	243	255	262	267	275
5600	0	204	220	232	240	243	250	257	263	270

In order to model engine speed the friction losses must be considered. As the engine speed increases the losses must increase so that when the fuel input is cut the engine speed decreases to the idle value. The friction losses are assumed linear.

The net torque of the vehicle is calculated by subtracting both the rolling resistance and the air drag load on the longitudinal axis (X-axis) of the body frame from the engine torque:

$$T_{NET} = T_{ENGINE} - T_{ROLLING\_RESISTANCE} - T_{AIR\_DRAG} \quad (2.3)$$

After calculating the net torque it is passes through the transmission system which is modeled next.

2.2.2 Transmission

As seen from Figure 8 an internal combustion engine does not provide a constant torque or power output. Both of them vary as the engine speed varies. However at an ideal engine one must have power constant no matter what the engine speed is [5]. The Power-Torque plot of an ideal engine is shown below:

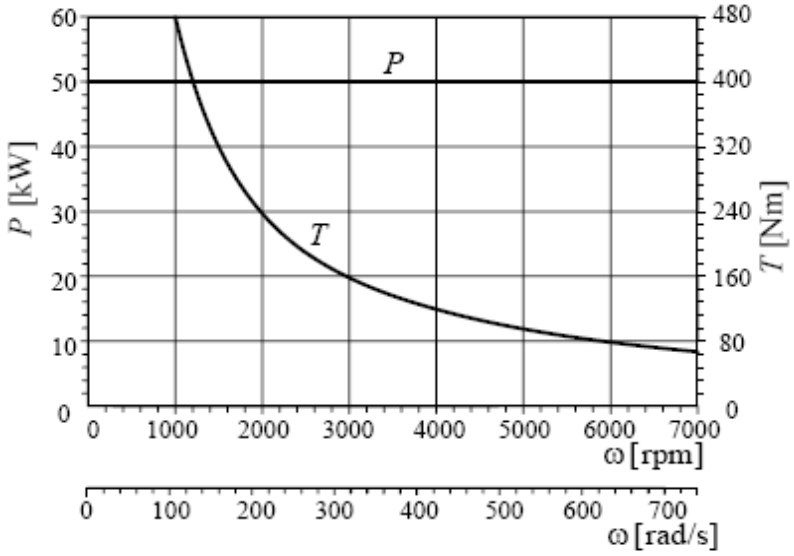

Figure 11 Ideal Engine Model with Constant Power and Decreasing Torque with Respect to Increasing Engine Speed [5].

The need for an ideal engine can be explained as follows: in order to have a comfortable ride it is needed to get the maximum power available from the engine at every engine speed (that points to an ideal engine as shown at Figure 11).

However this is not possible for a real engine due to its torque curve (Figure 8). In order to get the maximum power output for a certain amount of engine rpm, torque must be adjusted. Since the torque profile of an internal combustion engine cannot be changed to meet this criterion the transmission system is introduced to provide the necessary torque output for a larger band of the engine rpm such that when combined with the transmission the engine can be assumed ideal (Figure 12).

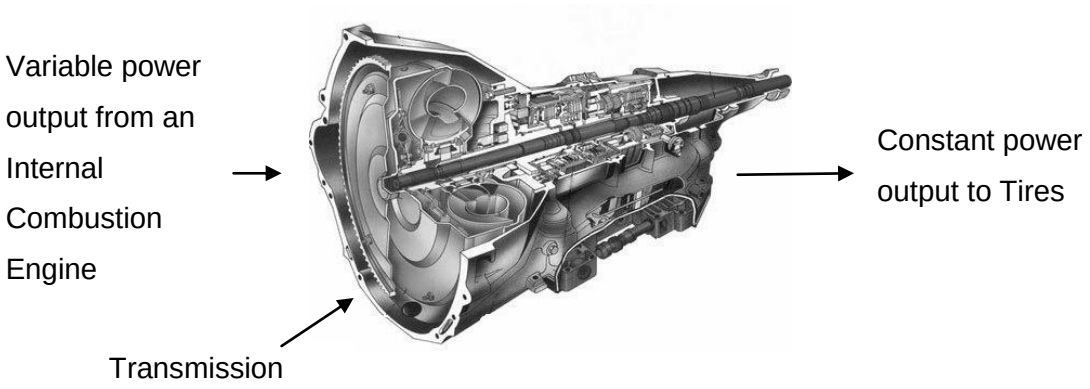

Figure 12 Role of the Transmission

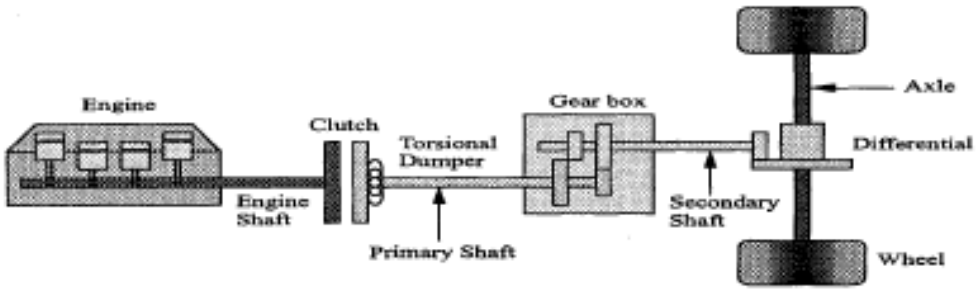

Figure 13 Coupled Engine and Transmission

In order to get the constant power output transmission introduces certain gear ratios to the torque of the engine output. Gears operate in such a way that increase in torque (T) output is inversely proportional with rotational speed (ω) output [9]. However for the given longitudinal speed the combination of the engine and the transmission approximates an ideal engine [5]. The effect of transmission coupled with an engine (Figure 13) is shown in the figure below:

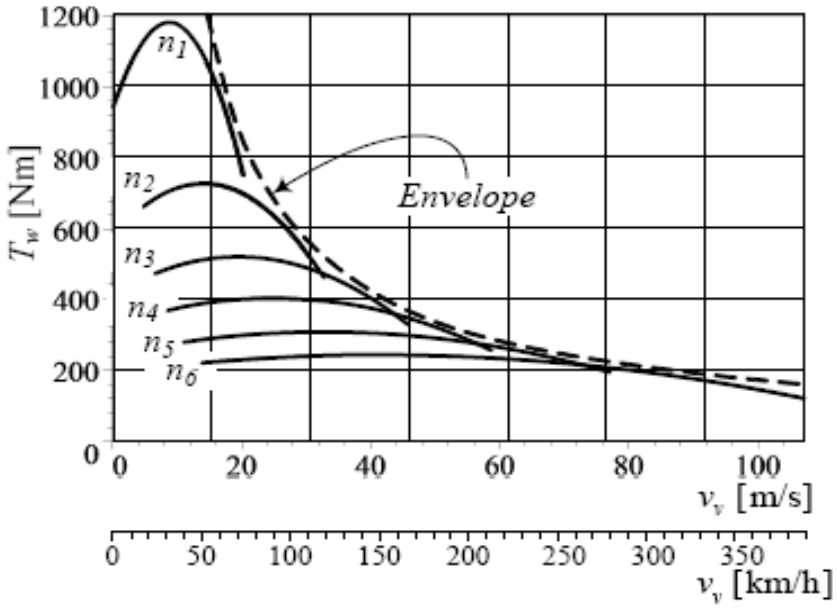

Figure 14 Torque Output of the Transmission Resembles an Ideal Engine by Creating a Torque Envelope [5].

The torque envelope is created by the transmission. The envelope is obtained with a selection of different gear ratios for selected longitudinal speed. The ratios are selected such that the engine speed band necessary for that longitudinal speed band is near the region of the maximum torque peak. When the longitudinal speed exceeds its allowed band the gear is changed and hence engine speed is changed for be preserved max torque region as well [9].

The transmission of the vehicle is chosen to be automatic in order to simplify the modeling of the transmission and decision making algorithm.

Such a gear ratio graph is given at Figure 15:

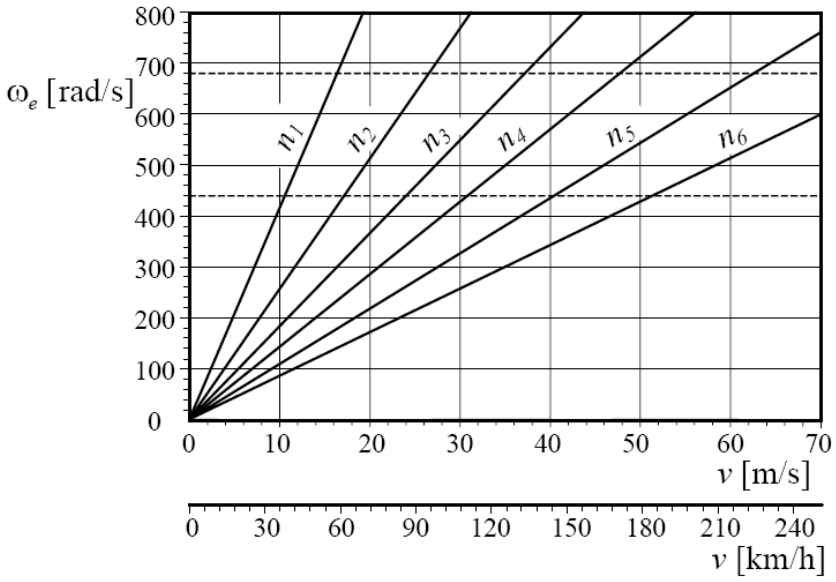

Figure 15 The Gear Ratios and Corresponding Regions for a Six Speed Gear for an Ordinary Car [5].

To further explain the process of gear change a simpler example can be given as follows. Consider a four gear transmission and an engine with a power vs. engine speed plot as given at Figure 16. In order to run this engine at the maximum power band (around 2800-5200 rpm) it is needed to keep the engine speed at this gap. To achieve this, the gear change algorithm should be such that for a given longitudinal speed the engine speed must be between these values (Figure 17).

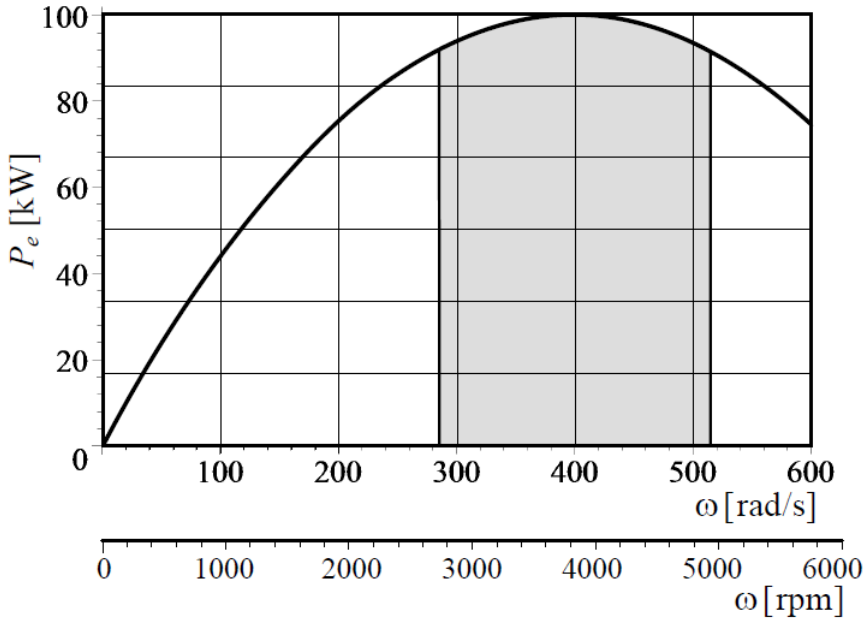

Figure 16 Power vs. Engine Speed Plot

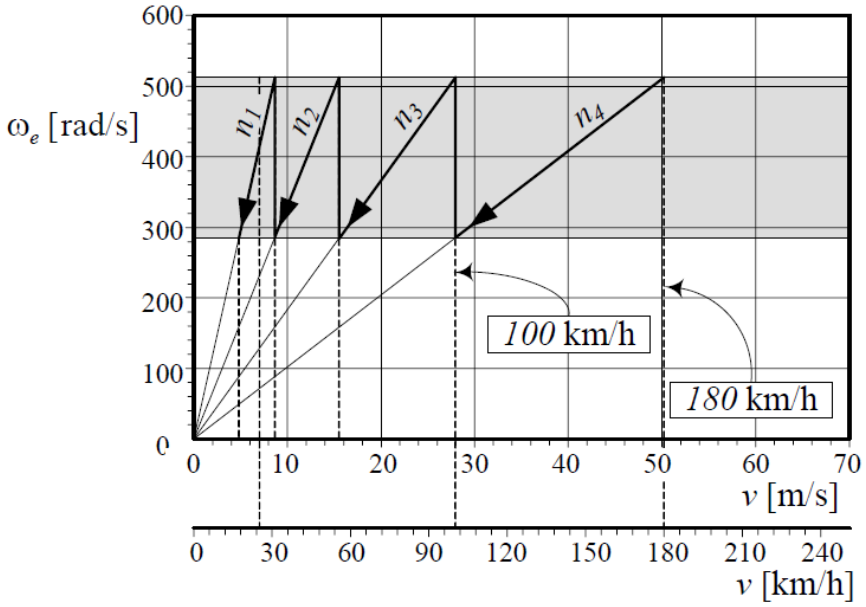

Figure 17 Gear Change Algorithm of the Given Example

In order to model a transmission a speed gear ratio algorithm is necessary to perform the mentioned changes. The algorithm for this job is a basic switch type one. In the simulation the gear changes occurs instantly.

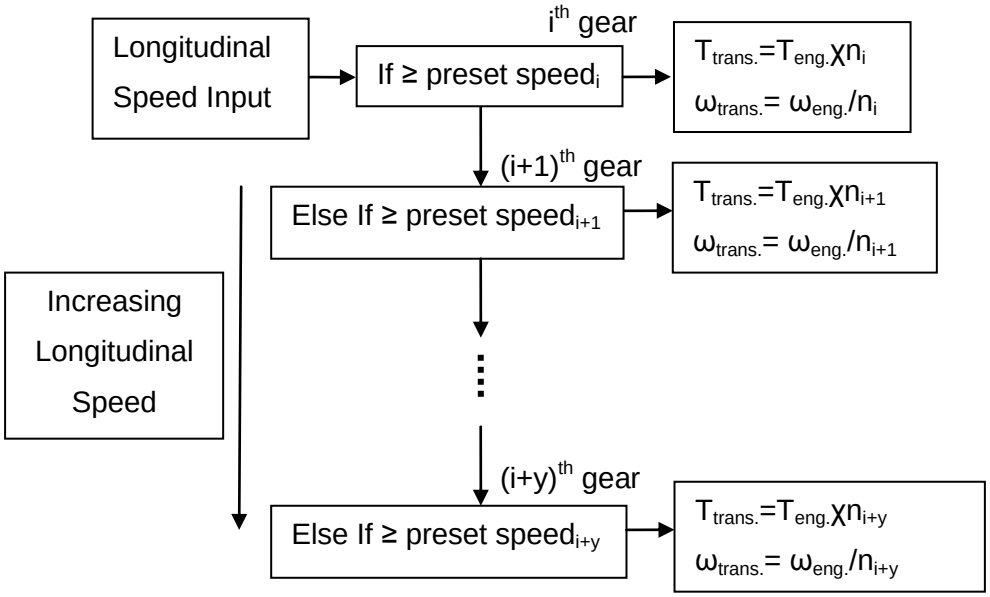

Figure 18 Automatic Transmission Algorithm

Table 2 Gear Ratios and their Corresponding Speeds

Gear Number	Gear Ratio	Change Speed of v_{bX} (m/s)
1	3.827	v_{bX} <6
2	2.36	6≤ v_{bX} <12
3	1.685	12≤ v_{bX} <18
4	1.312	18≤ v_{bX} <24
5	1	24≤ v_{bX} <32
6	0.793	v_{bX} ≥32

2.2.3 Tires

Tires are sources of friction for a car while it is moving. Tires both provide lateral and longitudinal friction [10]. Longitudinal friction forces convert the engine torque output to forward acceleration and lateral friction forces stabilizes the car along the body X-axis. The cornering stiffness forces that the front tires provide when the steering input is applied adjust yaw rate of the car (steering).

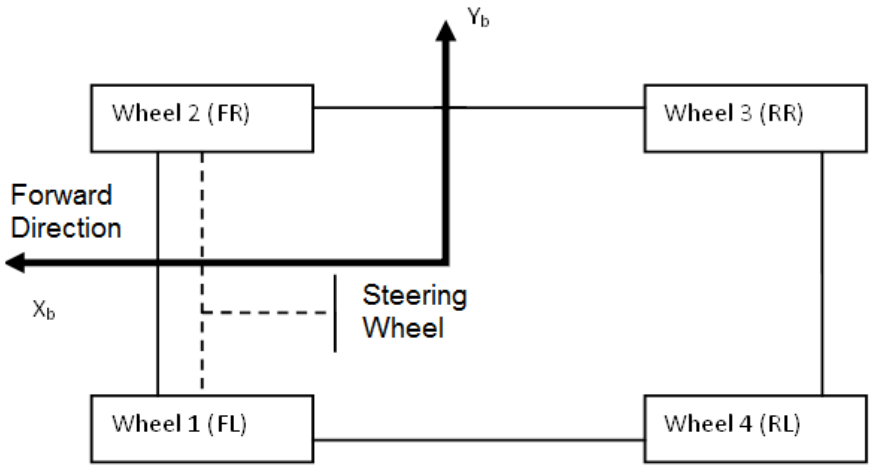

Figure 19 Planar View of a Car

As these friction forces cause the motion of the car each tire contributes to the net force in each of the car body axes. In order to find the net force we need to find the forces produced on each tire. After this step, adding the suspension forces will

give us all the net force a car is subjected to. The forces that are mentioned are shown on the figure below:

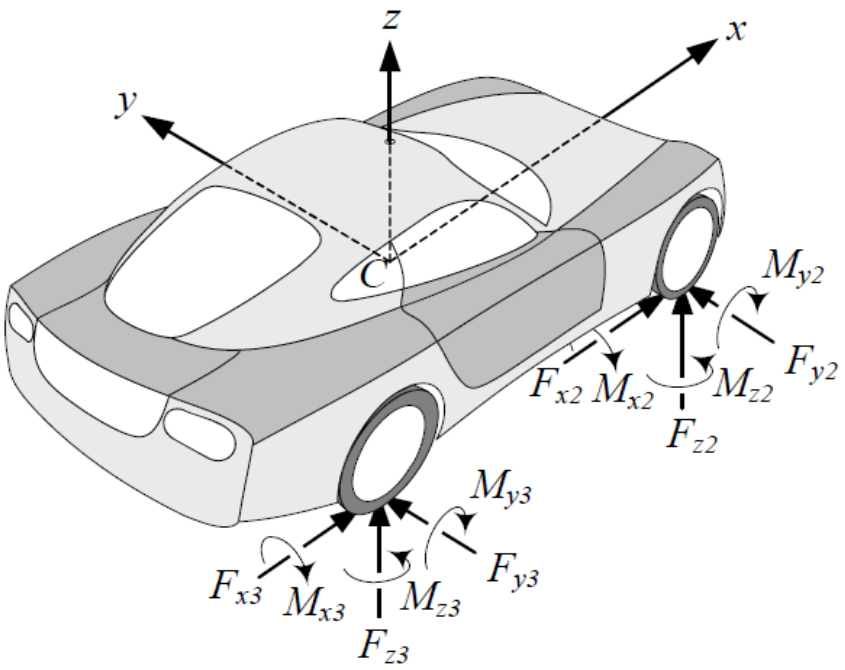

Figure 20 The Forces that Affect the Car can be Separated in Two Groups such as the Planar and Vertical Ones [5]

As it is seen from the figure above there are four longitudinal, four lateral and four vertical forces that a car is subjected. Separating the vertical ones (for the suspension part) we end up with the longitudinal and lateral ones. The figure below shows the dynamic profile of a tire:

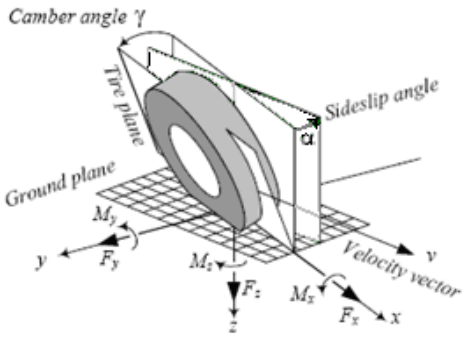

Figure 21 The Forces Generated at the Wheel. Sideslip Angle is Generated by Steering. Camber Angle is Neglected and Taken as Zero [5].

The yaw angle of the tire along the Z-axis is called tire sideslip angle and causes both a lateral force and a longitudinal force at tire body frame. The roll angle of the tire is called the camber angle and is assumed to be zero during this thesis work.

The sideslip angle of the tires is obtained by providing steering input. The change in sideslip angle causes the tire to produce a lateral force on the direction turned due to tires cornering force. This happens due to the friction forces which make the tire to change its shape (and the tire resistance to the change). The effect of cornering stiffness is shown below:

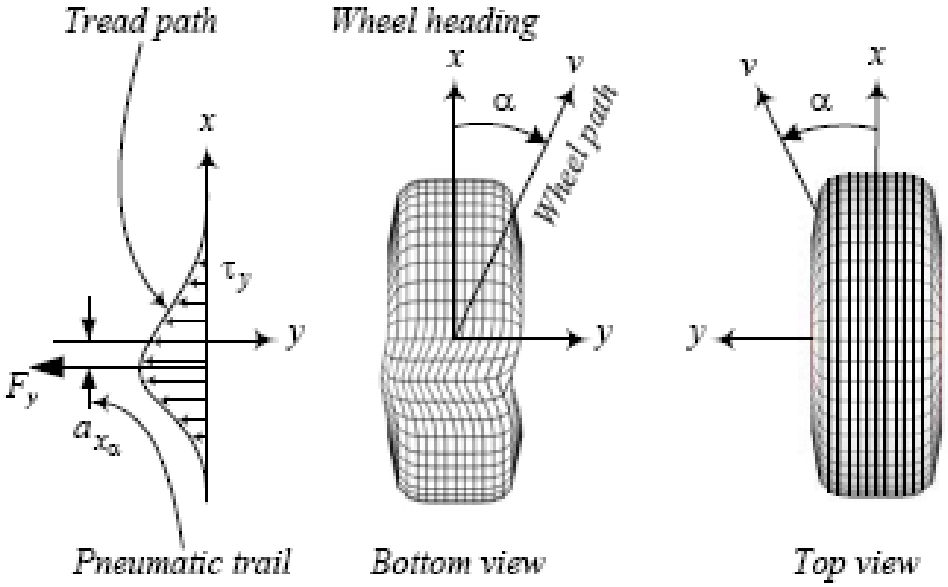

Figure 22 The Lateral Force Generation of a Wheel is Shown Above [5].

As mentioned before the rolling friction coefficient between rubber and asphalt is $\mu_{rolling}$ = 0.03 [12]. So for a 1000kg car the friction force becomes 300N. However the translational friction coefficient is μ_{trans} = 0.9 and it causes 9000N to move a car without tires rolling [13].

The formulation of “Cornering Stiffness” is given below:

$$F_{y\delta} = -C_\alpha \times \delta \tag{2.4}$$

The cornering force change linearly with sideslip angle of the tire up to 4° and then has a constant value. It is also affected from the vertical loading as both of them shown at below figures:

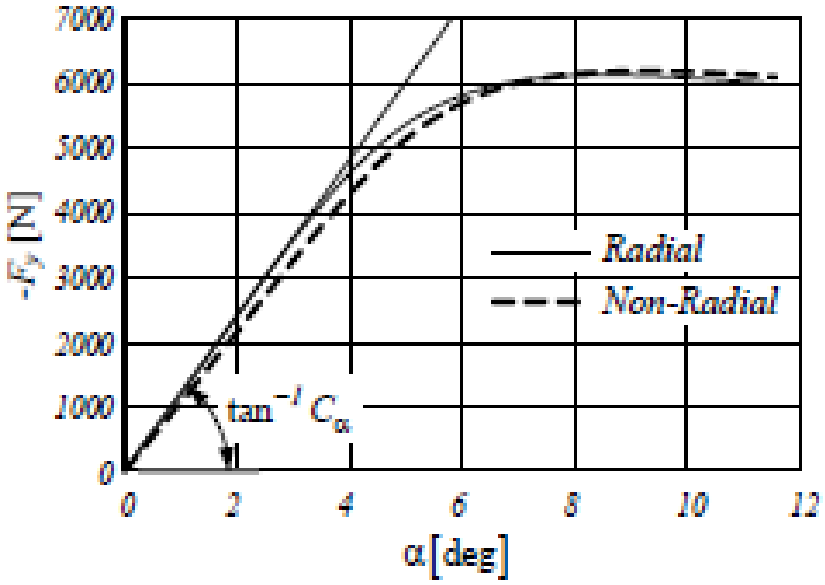

Figure 23 The Cornering Force of a Tire with Respect to its Type [5].

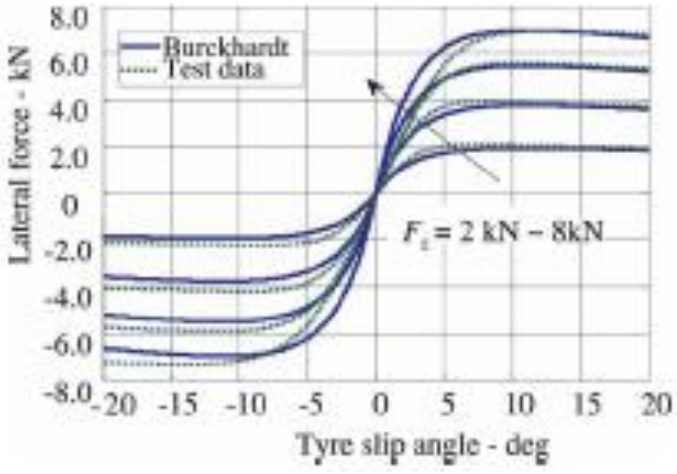

Figure 24 The Cornering Force of a Tire with Respect to its Vertical Loading [25].

However, since the linear change in the cornering stiffness due to sideslip is in a very narrow region (1°-6°), we can assume that it is constant through all sideslip

angles. Also the weight of the vehicle is assumed to be a point mass and all the tires are assumed to have the same load such that the cornering stiffness force is the same during motion with respect to the load.

By changing the sideslip angle of the tires via applying a nonzero steering input to them a non-zero value the cornering force is applied along lateral and longitudinal tire axis of the front tires. In order to formulate them the figure below is needed to show force vectors.

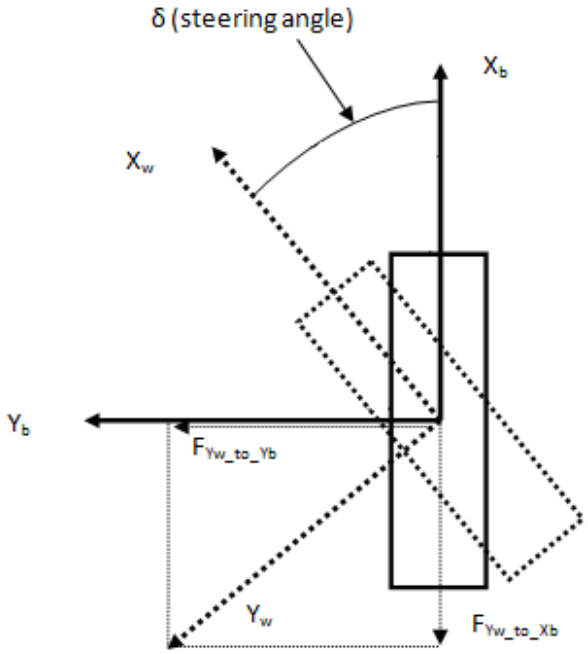

Figure 25 A Front Wheel Planar Forces Diagram Considering the Effects of Steering.

With the non-zero sideslip angle of a tire (which means the tire is rotated around its Z-axis) longitudinal and lateral force vectors of the tires turn as well at the same amount of sideslip angle value. However the quantity of the lateral force increases significantly because of the cornering stiffness. With the side slip longitudinal friction comes into consideration as well. The resulting force relation is given below [9]:

$$F_{Xi} = F_{xti}\cos\delta_i - F_{yti}\sin\delta_i \tag{2.5}$$

$$F_{Yi} = F_{yti}\cos\delta_i + F_{xti}\sin\delta_i \tag{2.6}$$

2.2.4 Steering Mechanism

The direction of the car is controlled by the steering wheel. By applying steering input to the front tires the sideslip angle of the front tires are changed and a lateral force is obtained there. Since the front tires are some distance from the center of gravity of the vehicle this lateral force acts as a torque on the vehicle body; hence causes it to change its yaw angle as well as forces it to accelerate in the lateral directions. However the lateral friction is translational and considerably higher than the steering force, so the lateral acceleration is negligible during longitudinal motion without cornering force.

There is a lot of steering principles-hence mechanisms- but the most frequently used one is the Ackermann Steering principle which is shown on the figures below:

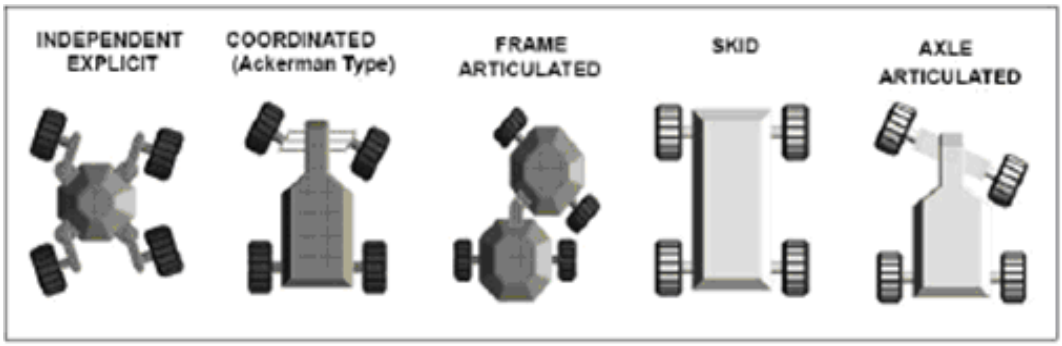

Figure 26 Steering Principles that are Used for Wheeled Land Vehicles [3]

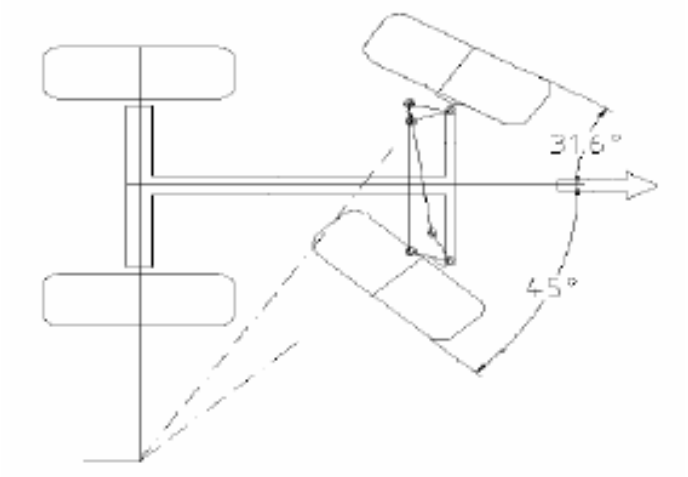

Figure 27 Detailed Figure of Ackermann Steering [3]

The Ackermann Steering is widely used in cars because it allows less stress on tires during turning; hence decreases turning radius and tire wear. Its drawback is its mechanical complexity since; in order to achieve the above objectives the sideslips of the inner and outer front tires must be different as seen on the figure above. The difference in angles minimizes the slip of the inner tire so that energy is conserved.

Beside its good features the complexity of the Ackermann Steering makes it difficult to model it. So in order to model the steering mechanism the Ackermann style is preserved while ignoring the angle difference between the front wheels so that both tires are assumed to have the same sideslip [14]. Since tire wear is not a concern in our simulations the only drawback of this assumption is wider turns than normal. The assumed steering mechanism is shown on the figure below:

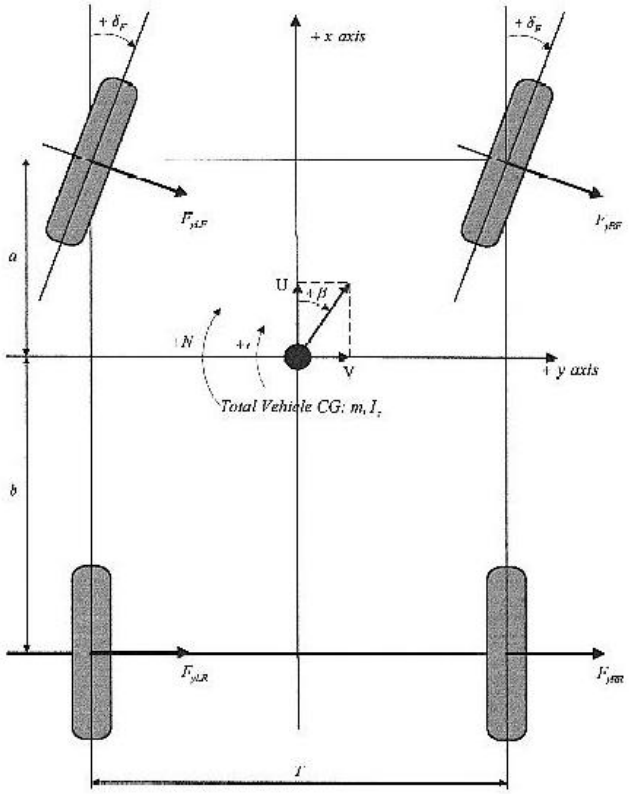

Figure 28 An Example of the Steering Mechanism Modeled In this Work [14].

2.2.5 Suspension

The suspension is the system that is designed for connecting the tires to the vehicle body in order to create a lumped system. The suspension absorbs shocks and damps the disturbances coming from the road. However it also affects the motion when the vehicle turns, accelerates and decelerates as the Center of Gravity of the car is higher than the tire height. As the vehicle body angles changes the affect of gravity also changes; so suspension modeling is an inevitable part of the model [10].

The suspension model of the vehicle is a spring-damper system as shown below. It is modeled as a 2nd order system of differential equations and are given below for front and rear axles [15].

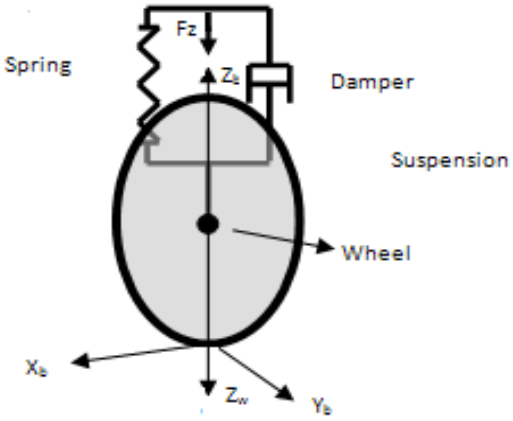

Figure 29 A Spring-damper Suspension System.

$$F_{z\_front} = 2K(a\theta + c\varphi - z) + 2C(a\dot{\theta} + c\dot{\varphi} - \dot{z}) \tag{2.7}$$

$$F_{z\_rear} = -2K(b\theta + c\varphi + z) - 2C(b\dot{\theta} + c\dot{\varphi} + \dot{z}) \tag{2.8}$$

The inputs for the suspention system are the z, $\dot{z}$, θ, $\dot{\theta}$, φ and $\dot{\varphi}$. The last four inputs are effected by the position of the wheel so that the distance from the CG must be multiplied in oder to calculate the force generation with these changing body angles. The car with complete suspension model will look like as shown in the figure below:

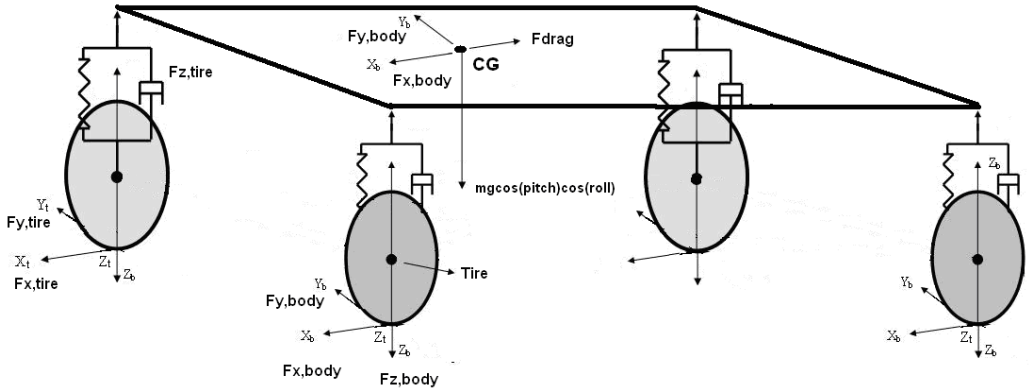

Figure 30 Car Model Including Suspensions [25]

2.2.6 Brakes

The brakes are for converting kinetic energy of the vehicle into heat energy and therefore decelerate the vehicle in its longitudinal axis. Since the vehicle cannot accelerate to the lateral axis without having a longitudinal speed it also decelerates the lateral movement but not independent from the longitudinal movement [5].

The cars generally have two types of brakes. One is drum brake and the other is disk brake. They operate with the same principle but with different mechanical principles. When activated both apply pressure to a rotating part to generate friction and slow down the vehicle until it stops [17]. They are shown on the figure below:

Figure 31 Disc Brake is Seen on the Left and Drum Brake is Seen on the Right

However modeling this process is complicated since this action is highly non-linear [4]. Considering the role of the brakes in a car they are modeled as torque providers in the negative direction of the motion of the car along body X-axis direction.

Each brake of the car provides a torque directly proportional to brake pedal angle (β):

$$F_{brake} = Tbrake \times \beta \times -\mathrm{sgn}(v_{bX}) \tag{2.9}$$

2.2.7 Slip

Slip is an important part of the car motion since it happens where the vehicle body and earth reference frame contact with each other. There are two types of slip.

One is the longitudinal slip and its cause is the deformation of the tire in longitudinal direction. The tire area in contact with the ground (tire print) produces two different friction coefficients. While the tire touches the ground the front contact area remains still for a small time interval and is considered static but the remaining part is sliding at the same instant hence considered moving. These two different contact areas can vary and hence produce different tire forces. The longitudinal slip determines the amount longitudinal force that can be converted to acceleration [4]. In our slip model the longitudinal slip is ignored which results in the fact that the longitudinal forces are transferred to the ground completely.

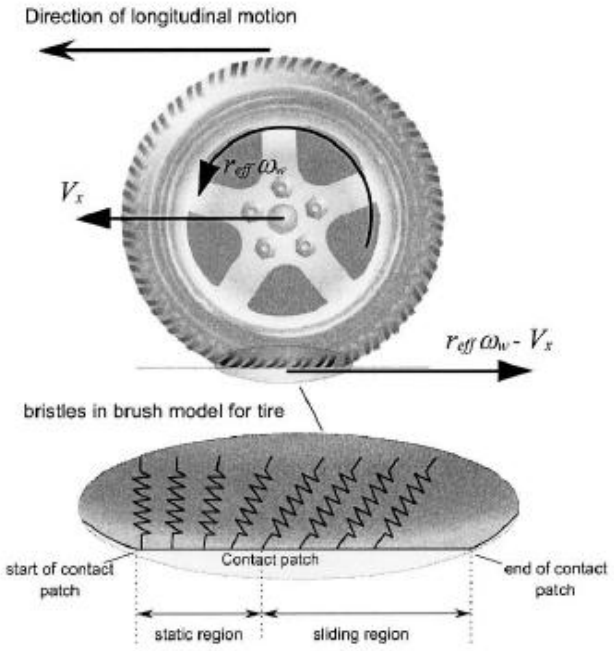

Figure 32 Longitudinal Slip [4]

The other slip type is the lateral slip. The tires slide when the lateral motion of the tire is different from the rotational speed times the longitudinal distance of the point that it is attached to. The lateral slip affects car's yaw angle hence its orientation, so it is considered important and included in the model [4].

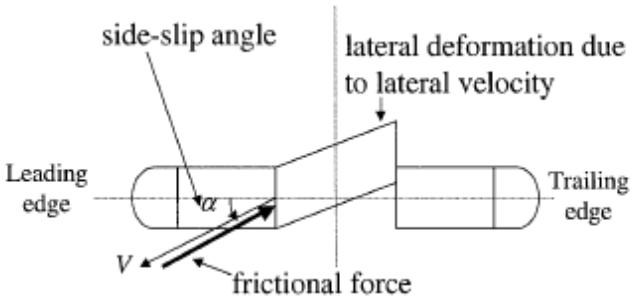

Figure 33 Lateral Slip [4]

The lateral forces caused by the lateral slip are calculated with respect to the equations below, assuming that slip angle of the tires are less than or equal to 4° [4]:

$$F_{y\_forward} = C_\alpha \left(\delta - \frac{v_{bY} + l_f \dot{\psi}}{v_{bX}} \right) \tag{2.10}$$

$$F_{y\_rear} = C_\alpha \left(- \frac{v_{bY} - l_r \dot{\psi}}{v_{bX}} \right) \tag{2.11}$$

2.2.8 Drag

As the cars go through air they are under the affect of drag inevitably. The air resistance makes the car to reduce its speed in the axes that the vehicle goes through translational motion. Without it the constant torque coming from the engine would make the car to reach very high speeds; so drag is the most important factor that limits the velocity of the vehicle [18].

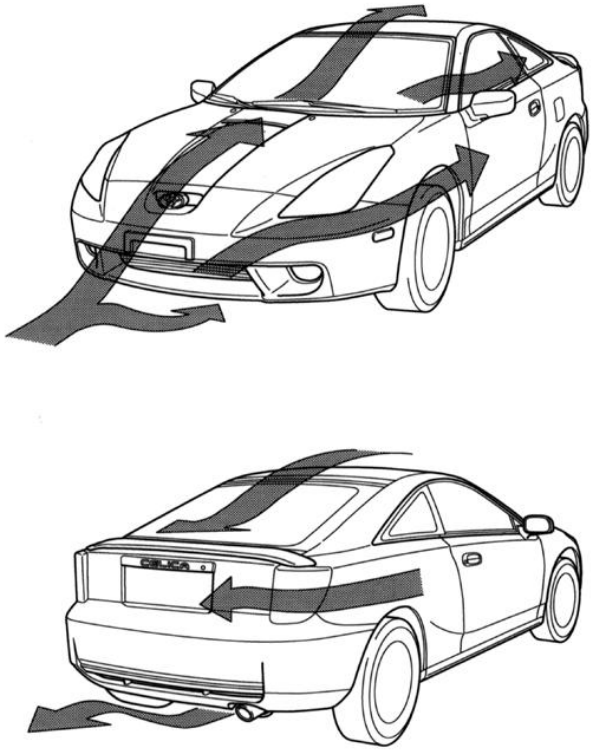

Figure 34 The Effect of Drag Force on a Car [17]

Since the car model will be move along its longitudinal and lateral axes it will face two different drag forces. But it should be noted that lateral and longitudinal axes have different contact areas (A) and aerodynamic drag coefficients (C_d).

The calculation of drag force is done with respect to the following equation [18]:

$$F_D = 0.5\rho v^2 C_d A \tag{2.12}$$

(ρ is air density and 1.239 kg/m^{3,}, C_d is drag coefficient, v is the velocity along drag axis and A is the area where drag force is generated)

CHAPTER 3

6DOF DYNAMIC VEHICLE MODEL

The dynamic vehicle model will be in six dimensions namely X, Y, Z, and Roll (Φ), Pitch (θ) and Yaw (ψ) axes. The model includes six equations.

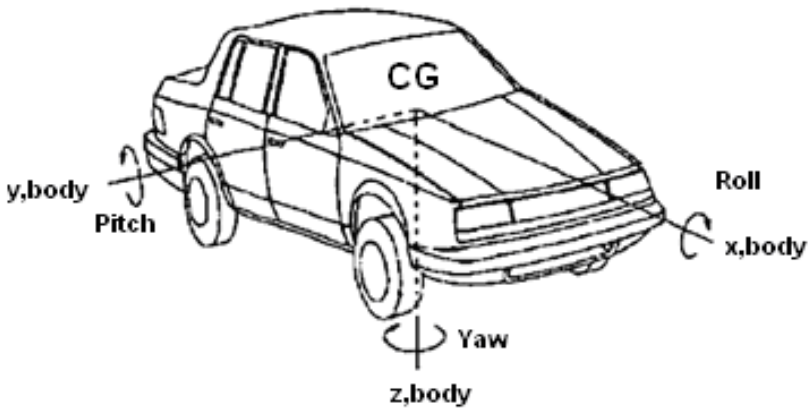

Figure 35 Axes of the 6DoF Dynamic Model

3.1 X-Axis

The X-Axis is the longitudinal axis. The vehicle is affected from the tire forces along the X-Axis. Also gravity is important and it is affected from the sine of the pitch (θ) value of the vehicle body frame. The axis is also affected from the drag along the longitudinal direction. A figure about motion in X-Axis is given below:

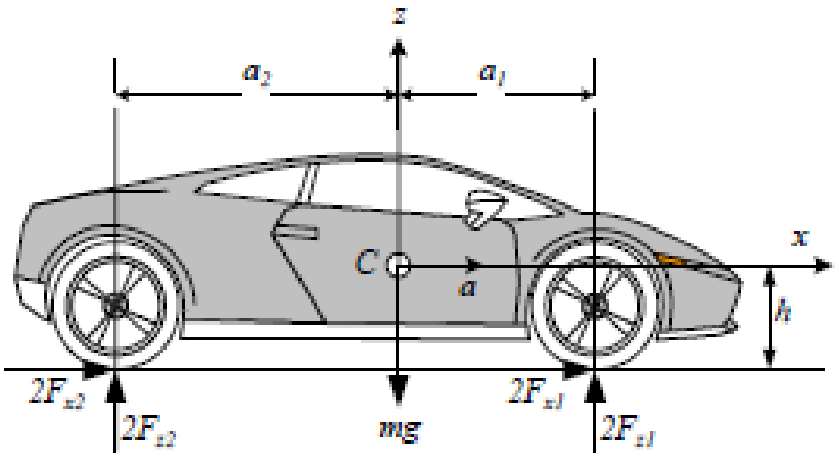

Figure 36 Forces Acting on the X-Axis [5]

As seen from the figure net tire force in the X-Axis are added to the drag and gravity forces to produce the motion along the X-Axis. Due to Euler angles the X-Axis in the Body Reference frame must be converted to the Earth Reference frame to calculate the exact position of the vehicle. Hence the final equation is given below [20]:

$$m(\dot{u} + \omega_y w - \omega_z v) = \sum F_{xi} + mg\sin\theta + F_{drag\_x} \tag{3.1}$$

3.2 Y-Axis

The Y-Axis is the lateral axis. The vehicle is affected from the tire forces along the Y-Axis. Also gravity is important and it is affected from the sine of the roll (Φ) value ad cosine of the pitch (θ) value. The axis is also affected from the drag along the lateral direction. A figure about motion in Y-Axis is given below:

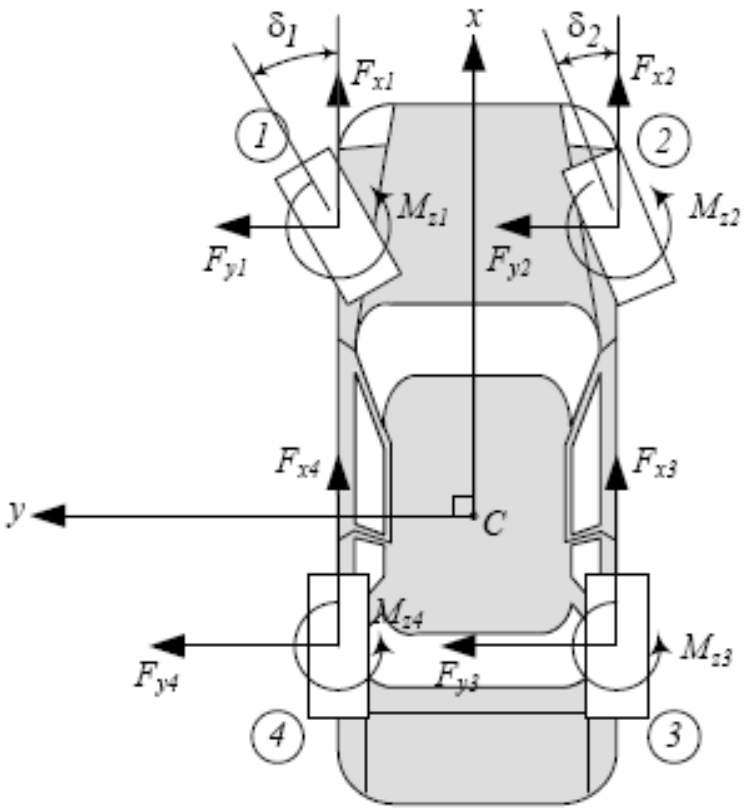

Figure 37 Forces Acting on the Y-Axis (Except Gravity and Drag) [5]

As seen from the figure net tire force in the Y-Axis are added to the drag and gravity forces to produce the motion along the Y-Axis. Due to Euler angles the Y-Axis in the Body Reference frame must be converted to the Earth Reference frame to calculate the exact position of the vehicle. Hence the final equation is given below [20]:

$$m(\dot{v} + \omega_z u - \omega_x w) = \sum F_{yi} - mg \sin\varphi \cos\theta + F_{drag\_y} \qquad (3.2)$$

3.3 Z-Axis

The Z-Axis is the vertical axis. The vehicle is affected from the suspension forces along the Z-Axis. Also gravity is important and it is affected from the cosine of the roll (Φ) value and cosine of the pitch (θ) value. A figure about motion along Z-Axis is given below:

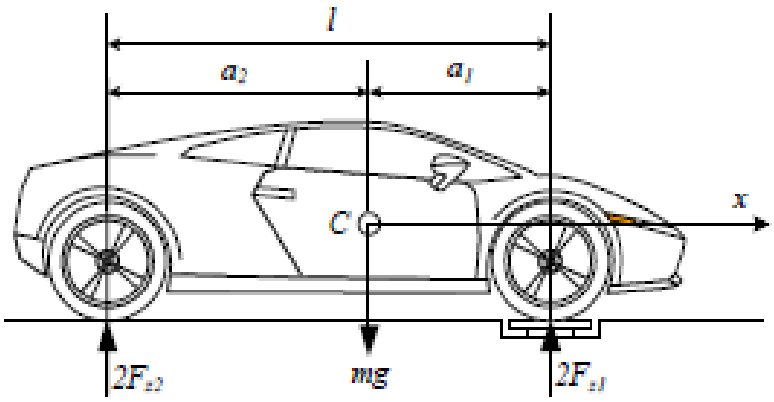

Figure 38 Forces Acting on the Z-Axis [5]

As seen from the figure net tire force along the Z-Axis are added to the gravity force to produce the motion along the Z-Axis. Due to Euler angles the Z-Axis in the Body Reference frame must be converted to the Earth Reference frame to calculate the exact position of the vehicle. Hence the final equation is given below [19]:

$$m(\dot{w}+\omega_x v-\omega_y u)=\sum F_{zi}-mg\cos\varphi\cos\theta \tag{3.3}$$

3.4 Roll

The Roll motion is the rotational position change of the vehicle around its X-Axis. The vehicle is affected from the suspension forces in the Z-Axis. The suspension forces are multiplied with the distance of the suspensions to the X-Axis so that the moment values can be calculated. A figure about roll motion is given below:

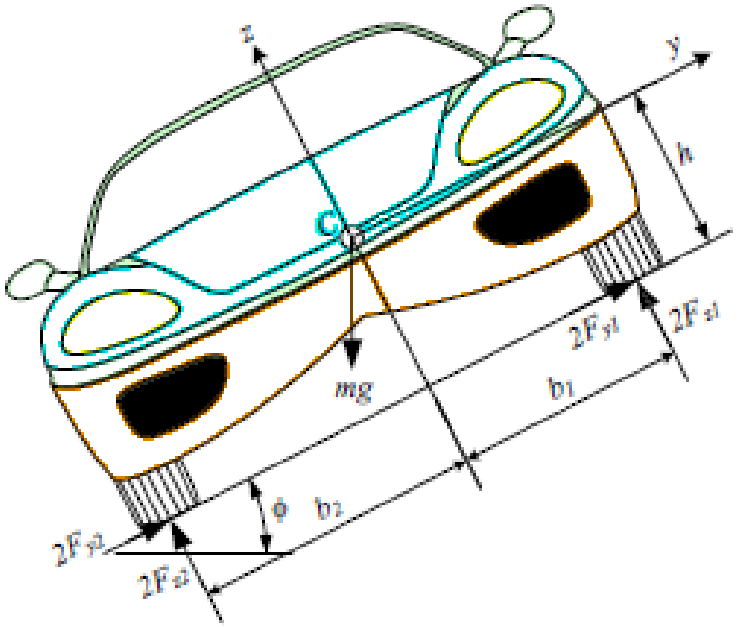

Figure 39 Forces Acting on the Roll Motion [5]

As seen from the figure suspension forces in the Z-Axis are multiplied with their leverage to convert them to torque and they are added in order to produce the roll motion around the X-Axis. Body reference frame roll motion does not differ from the Earth reference frame roll motion. So no conversion is needed. Hence the final equation is given below [20]:

$$J_x \dot{\omega}_x = \frac{c(F_{z1} + F_{z4} - F_{z2} - F_{z3})}{2} \tag{3.4}$$

(c is the distance between tires in the Y-Axis)

3.5 Pitch

The Pitch motion is the rotational position change of the vehicle around its Y-Axis. The vehicle is affected from the suspension forces in the Z-Axis. The gravity is not included since it cancels itself due to not having leverage. The suspension forces are multiplied with the distance of the suspensions to the Y-Axis so that the torque values can be calculated. A figure about roll motion is given below:

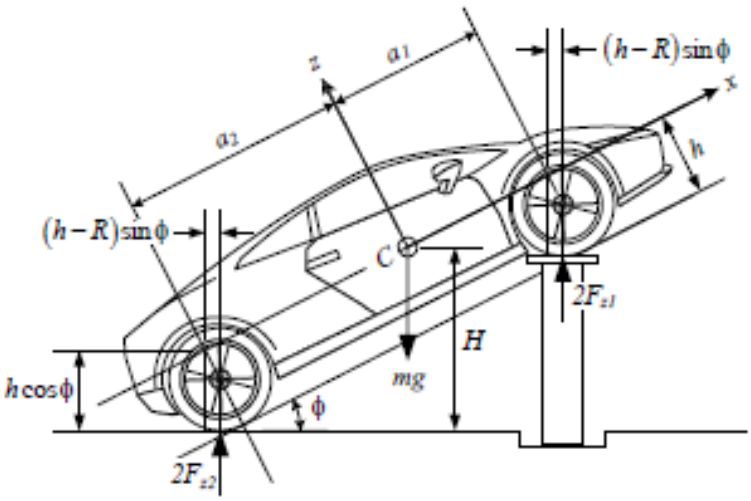

Figure 40 Forces Acting on the Pitch Motion [5]

As seen from the figure suspension forces in the Z-Axis are multiplied with their leverage to convert them to torque and they are added in order to produce the pitch motion around the Y-Axis. Body reference frame pitch motion does not differ from the Earth reference frame pitch motion. So no conversion is needed. Hence the final equation is given below [20]:

$$J_y \dot{\omega}_y = b(F_{z3} + F_{z4}) - a(F_{z1} + F_{z2}) \tag{3.5}$$

(b is the distance of the rear tires to the Y-Axis, a is the distance of the front tires to the Y-Axis)

3.6 Yaw

The Yaw motion is the rotational position change of the vehicle around its Z-Axis. The vehicle is affected from the planar forces along the X-Axis and Y-Axis. The gravity is not included since it cancels itself due to not having leverage. The longitudinal forces are multiplied with the distance of them to the X-Axis and the lateral forces are multiplied with the distance of them to the Y-Axis in order to calculate the torque values. A figure about yaw motion is given below:

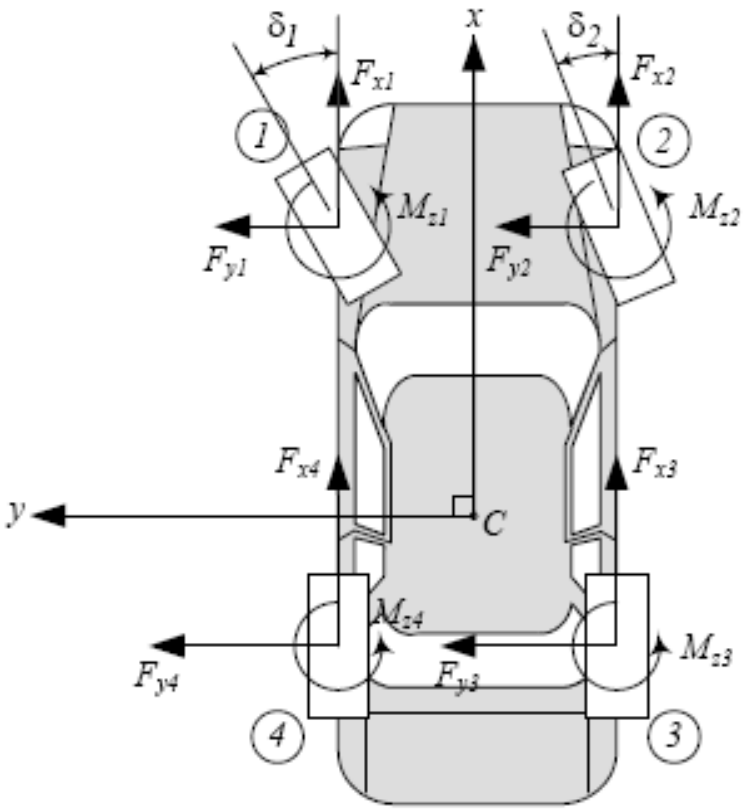

Figure 41 Forces Acting on the Yaw Motion [5]

As seen from the figure longitudinal forces in the X-Axis are multiplied with their leverage to convert them to torque as well as the lateral ones with their leverage to the Y-Axis. Then they are added in order to produce the yaw motion around the Z-Axis. Body reference frame yaw motion does not differ from the Earth reference frame yaw motion. So no conversion is needed. Hence the final equation is given below [20]:

$$J_z\dot{\omega}_z = a(F_{y1}+F_{y2}) - b(F_{y3}+F_{y4}) + \frac{c}{2}(-F_{x1}+F_{x2}-F_{x4}+F_{x3}) \qquad (3.6)$$

3.7 Model Summary

The summary of the all six equations are listed below [20]:

1. $m(\dot{u}+\omega_y w-\omega_z v)=\sum F_{xi}+mg\sin\theta+F_{drag\_x}$ (3.1)
2. $m(\dot{v}+\omega_z u-\omega_x w)=\sum F_{yi}-mg\sin\varphi\cos\theta+F_{drag\_y}$ (3.2)
3. $m(\dot{w}+\omega_x v-\omega_y u)=\sum F_{zi}-mg\cos\varphi\cos\theta$ (3.3)
4. $J_x\dot{\omega}_x=\frac{c(F_{z1}+F_{z4}-F_{z2}-F_{z3})}{2}$ (3.4)
5. $J_y\dot{\omega}_y=b(F_{z3}+F_{z4})-a(F_{z1}+F_{z2})$ (3.5)
6. $J_z\dot{\omega}_z=a(F_{y1}+F_{y2})-b(F_{y3}+F_{y4})+\frac{c}{2}(-F_{x1}+F_{x2}-F_{x4}+F_{x3})$ (3.6)

Table 3 Vehicle Physical Features

Vehicle Information		
Feature	Explanation	Value
a	Longitudinal distance of front tires to CG	1m
b	Longitudinal distance of rear tires to CG	1.6m
c	Lateral distance of tires to CG	0.7m
J_X	Moment of inertia in x-axis	600kgm^2
J_y	Moment of inertia in y-axis	3500kgm^2
J_z	Moment of inertia in z-axis	3000kgm^2
m	Car mass	1200kg

CHAPTER 4

AUTOPILOT

An autopilot for the vehicle system is designed to control the car in order to follow given waypoints. To achieve this goal the following parts are required to be designed:

1. A navigation part to decide the direction and distance to the given waypoint and current position and activate brakes,
2. A controller for the steering input in order to control the yaw angle so the car goes along the desired direction,
3. A controller for the throttle input so that the car follows the desired speeds on the current course,
4. A brake activator to stop the vehicle when it comes the last way point.

The plot of such a system is given at the below figure:

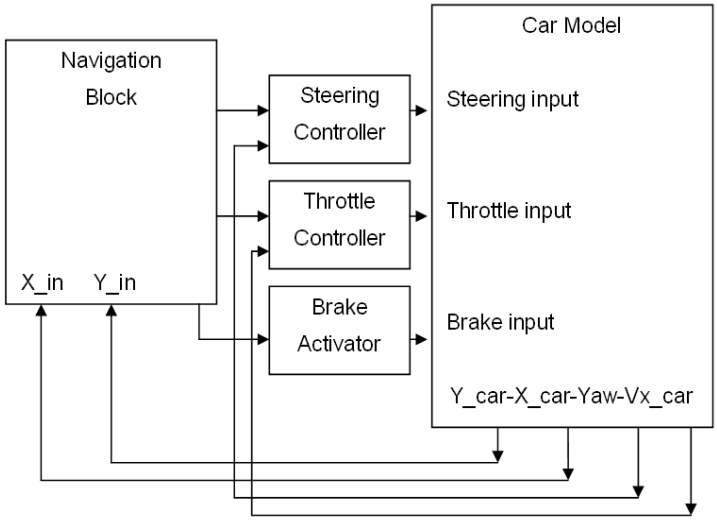

Figure 42 Designated Autopilot Structure for the Model

4.1 Design of Navigation Block

The Navigation block has three goals to achieve:

1. Comparing the current position with the desired waypoint to decide the steering input to the steering controller,
2. Comparing the current position with the desired waypoint to decide the remaining distance,
3. To stop the car when the track is completed.

In order to achieve these goals the navigation block takes current X and Y position of the vehicle with respect of the Earth reference frame. Also it stores a given number of waypoints and tracks them one after the other by stepping to the next waypoint as the vehicle reaches the current one. It performs this duty until all of the waypoints are reached with their respective order. The plot of the navigation system is given on the figure below:

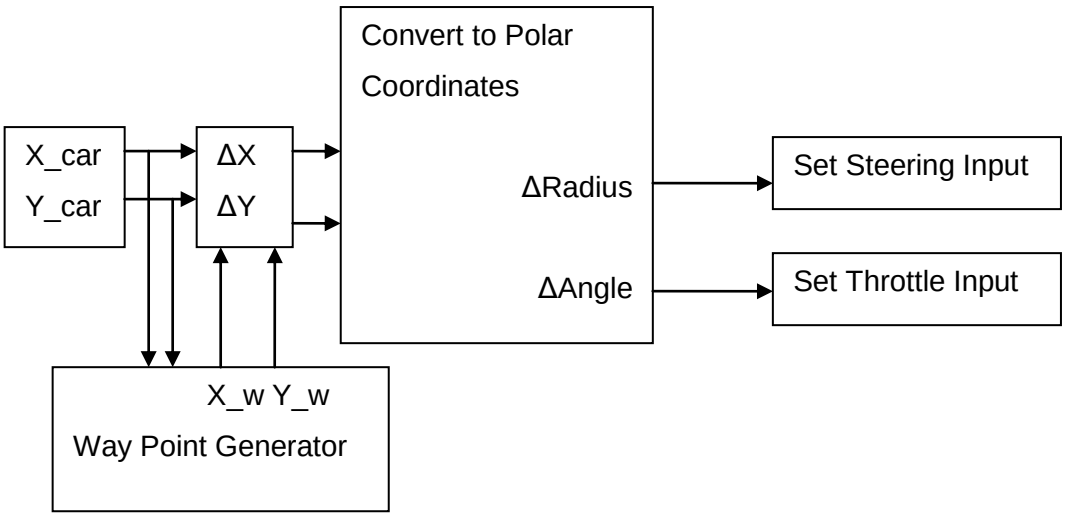

Figure 43 Schematic of the Navigation Block

4.2 Design of PID (Proportional-Integral-Derivative) Controllers

The basic but reliable PID (proportional-integral-derivative) controllers are chosen to be used in the simulations in order to minimize controller errors and detect model faults. Due to their reliability, ease of design and ability to tune the system after implementation the PID controllers are widely favored among controller engineers. The theory of PID controllers is as follows. The controller has a set point that is desired to be reached (for servo systems) or be stayed (for regulator systems). The PID controller takes the output and subtracts it from the set point to calculate the error signal. After obtaining the error signal it puts the error signal as the input to proportional, integral and derivative blocks to calculate the reaction to decrease the magnitude of the error signal [11]. The functions of these blocks are given below:

1. At the proportional block the reaction against current error signal is determined.
2. At the integral block the reaction against the recent sum of error is determined.
3. At the derivative block the reaction against the changing rate of error is determined.

After these reactions are calculated, they are added as a weighted sum and the output value is given to the plant as the control input. The transfer function of the PID controller in frequency-domain is given below [21]:

$$G_C(s) = K_P + \frac{K_I}{s} + K_D \cdot s \tag{4.1}$$

To construct the controller three constants are needed:

1. "K_P" proportional constant,
2. "K_I" integration constant,
3. "K_D" derivative constant.

The equation for the controller output in the time-domain is

$$u(t) = K_P e(t) + K_I \int e(t)dt + K_D \frac{de(t)}{dt} \tag{4.2}$$

where K_P is the “proportional gain”, K_I is the “integral gain”, K_D is the “derivative gain” and e(t) is the “error signal” [21].

The general PID configuration is given below:

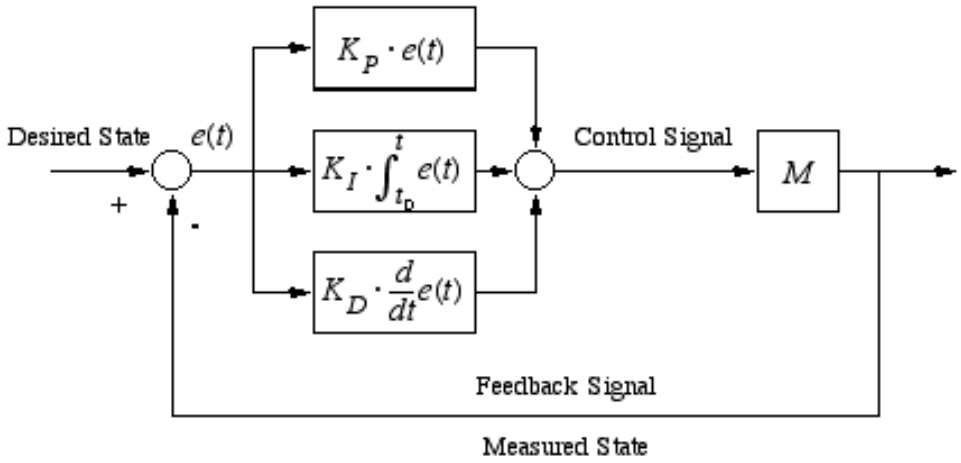

Figure 44 Generic PID Scheme with M is the Plant and e(t) is the Error Signal [22]

4.3 Design of the Steering Controller Block

The Steering controller is the main controller for the system since the vehicle reaches the designated waypoints via this controller. It is a PID controller and takes the cars yaw value and the desired yaw value for the way point to head as its inputs. It subtracts them from each other and finds the yaw error and puts this error signal to the PID controller and collects PID’s output. The collected controller

output is also is passed through a saturation block to limit the maximum amount of steering between ±10°, since a car cannot steer more than that value.

The designed PID controller for the steering controller has the following requirements for a vehicle going at a constant speed of 40km/h and a 10° degree steer:

- Rise time should be less than 3 seconds,
- Percentage overshot for the step input should be less than 1%,
- Settling time should be less than 5 seconds,
- Steady-state error should be less than 1%.

The designed controller parameters are given below.

- K_P=32.567
- K_I=5.186e-003
- K_D=10.755

The performance of this controller is shown on the figure below:

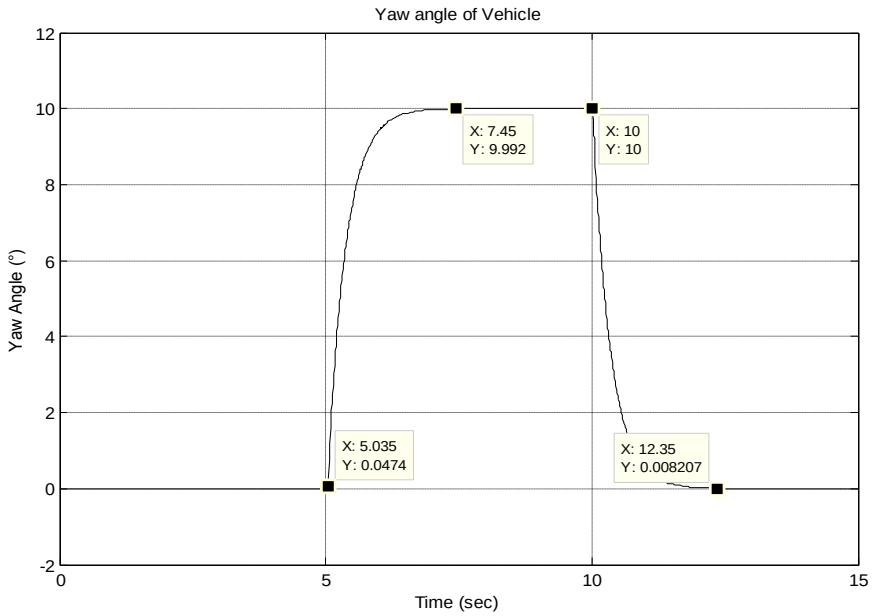

Figure 45 Steering Performance of the Car at 40km/h with a 10° Steering Angle

4.4 Design of the Throttle Controller Block

The throttle controller is the other controller for the system as it is responsible for the longitudinal velocity of the vehicle. The vehicle longitudinal speed has to be controlled in order to control the turns since inadequate speeds can cause inefficient turns or missing waypoints. The throttle controller is a PID controller and accepts the cars longitudinal speed in body reference frame and the preset speed value determined by the distance to the way point as its inputs. It subtracts them from each other and finds the speed error and inserts this error signal into the PID controller and obtains its output. The controller output is also passed through a saturation block to hold the amount of the throttle value between 0 and 1, since they are the range limits of a full sweep throttle pedal.

The designed PID controller for the throttle has the following requirements for a vehicle that is at 0km/h to reach a constant speed of 100km/h and a 0° degree steer:

- Rise time should be less than 10 seconds,
- Percentage overshot for the step input should be less than 5%,
- Settling time should be less than 15 seconds,
- Steady-state error should be less than 1%.

The designed controller coefficients are given below:

- K_P= 5.342e3,
- K_I= 6.4001e4,
- K_D= 2.2343e6.

The performance of this controller is shown on the figure below:

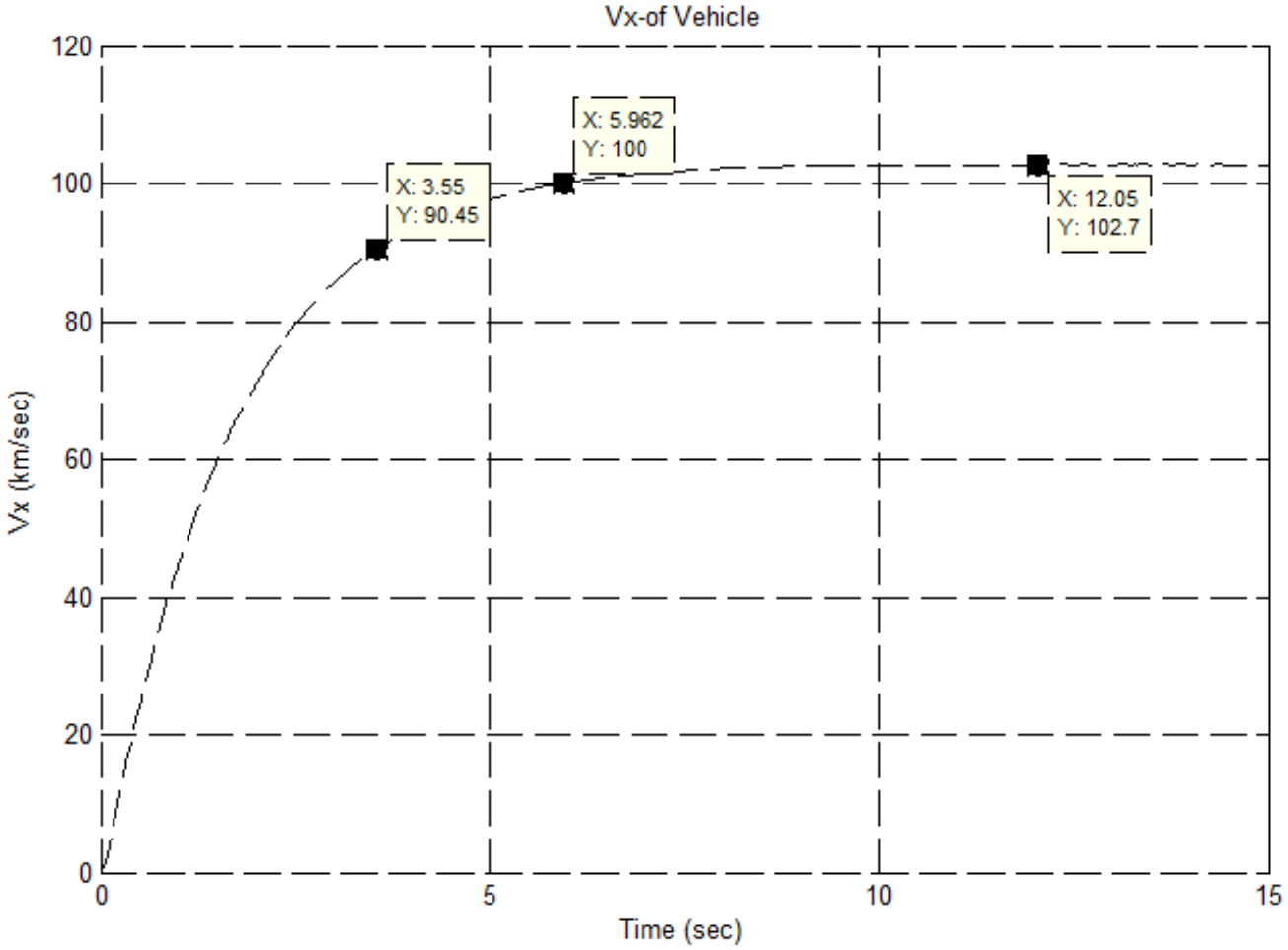

Figure 46 Speeding Performance of the Car From 0km/h to 100km/h with a 0° Steering Angle

4.5 Design of the Brake Activator

The brakes of the system enable it to decelerate and stop at a given waypoint. The brake activator's duty is to stop the vehicle at a given waypoint. It can also decelerate the vehicle. In the simulation the brakes are linked to the throttle since activating both the engine and the brakes are not practical. For the closest stop time and distance the engine should not give any torque input to the tires.

The designed brake activator for the braking action has the following requirements for a vehicle that is at 57km/h to and a 0° degree steer value to stop:

- Time needed to stop the vehicle should be less than 10 seconds.

Looking at the graph for the braking action, it is seen that the brakes are activated when the vehicle was at a steady speed of 57km/h at t = 15 sec and the vehicle reach 1.4km/h (which is assumed to be approximately zero for the simulation) at 24.3 sec.

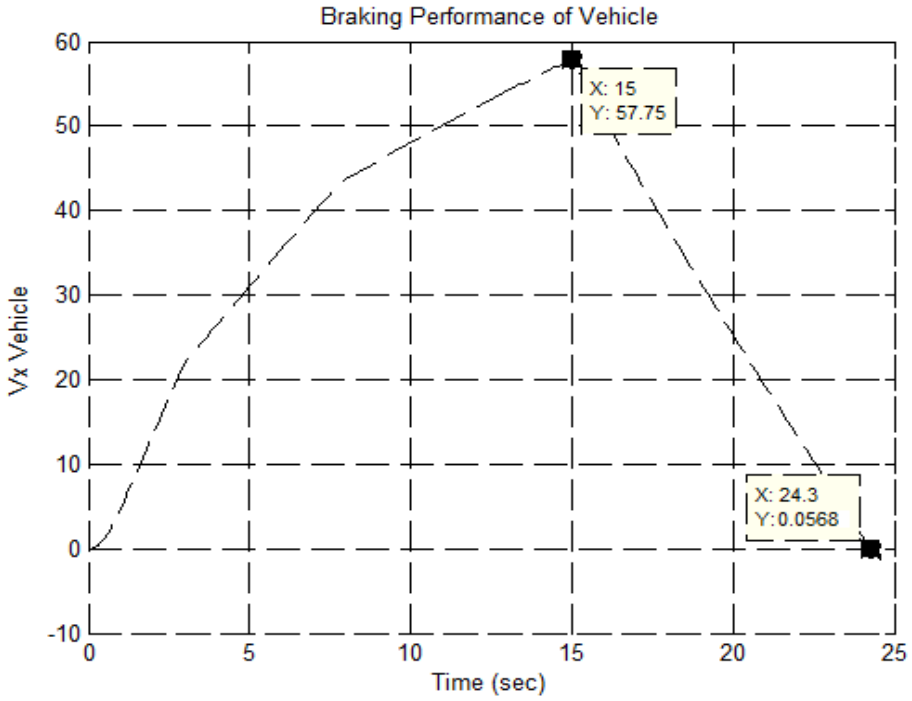

Figure 47 Performance of Brakes

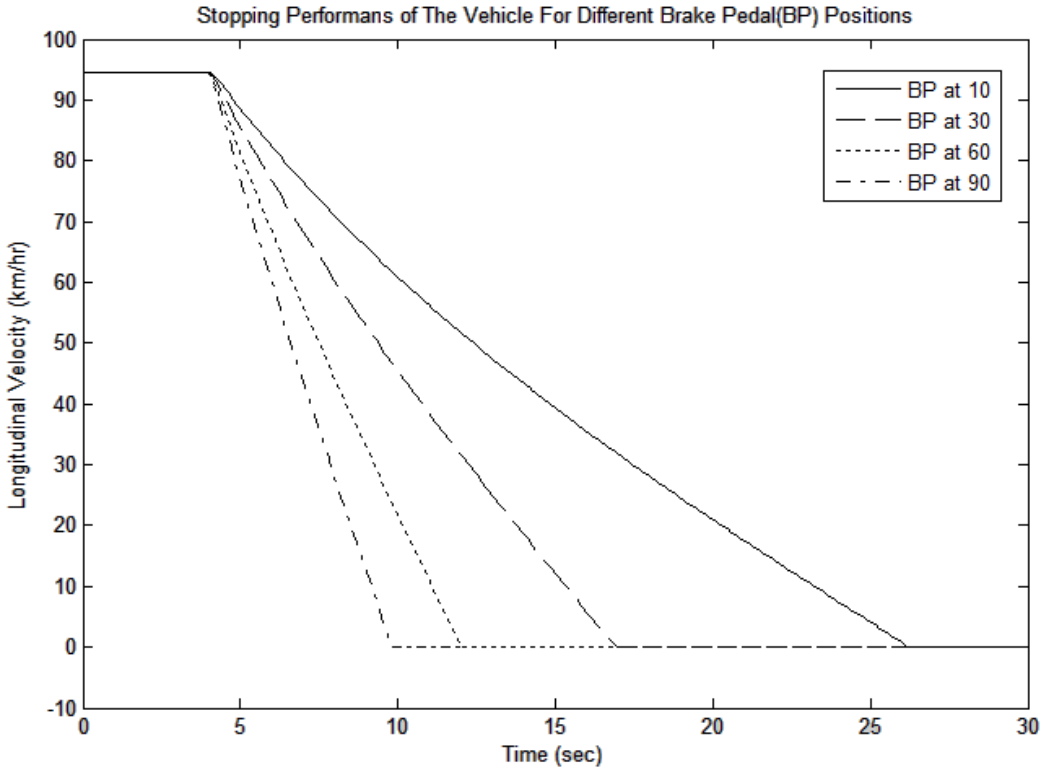

Figure 48 Stopping Performance of the Vehicle for Various Braking Pedal Positions

4.6 Simulation Results of the Model

In order to evaluate the model some simulations are performed. During these simulations the model was run for different test maneuvers. The first simulation has a waypoint list as given below:

Table 4 List of Waypoints for Simulation

Waypoint#	X_desired (m)	Y_desired (m)
Initial	0	0
1	100	0
2	100	20
3	100	40
4	100	100

The vehicle course ends in 25sec. and it went nearly 200m. The car started at (0,0) and went to the next waypoint as soon as it got within 5m to the current one

and stopped at the last one situated at (100,100). The resultant path of the vehicle together with the desired path is given below:

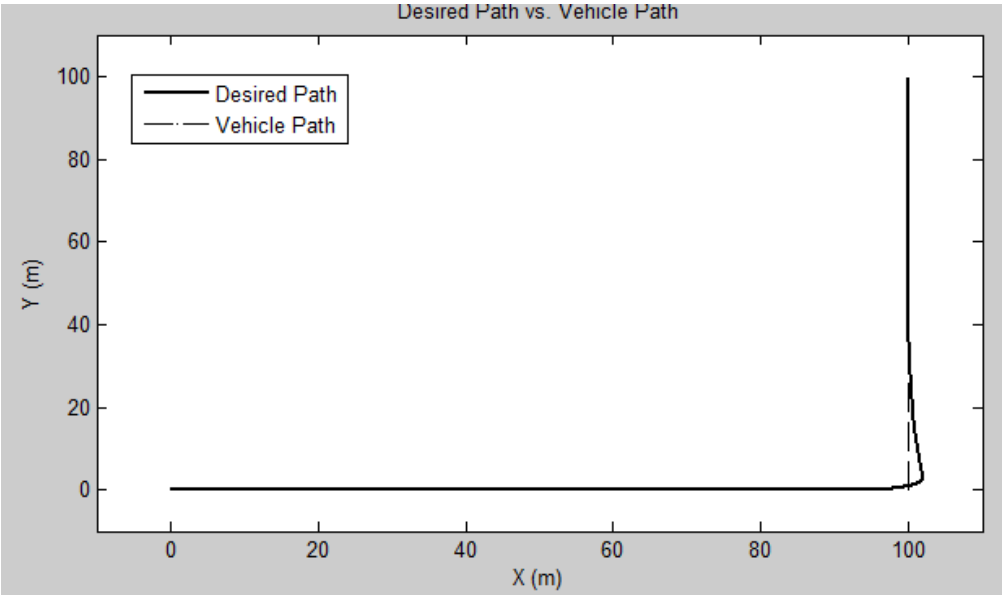

Figure 49 Desired Path and the Actual Path of the Car

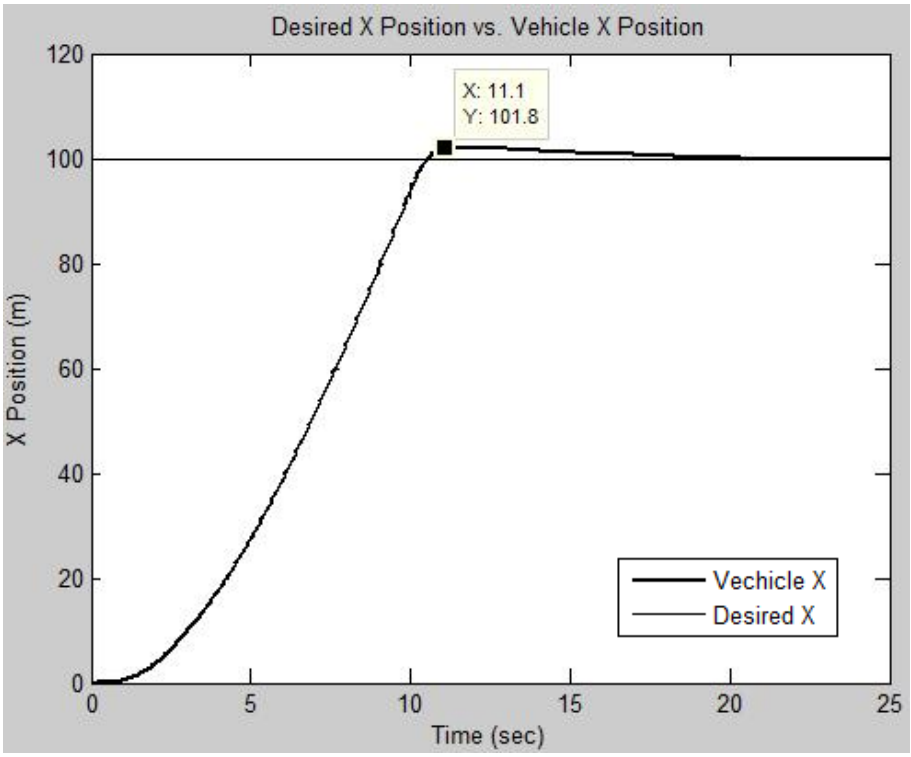

Figure 50 Desired X Position vs. Actual X Position of the Vehicle

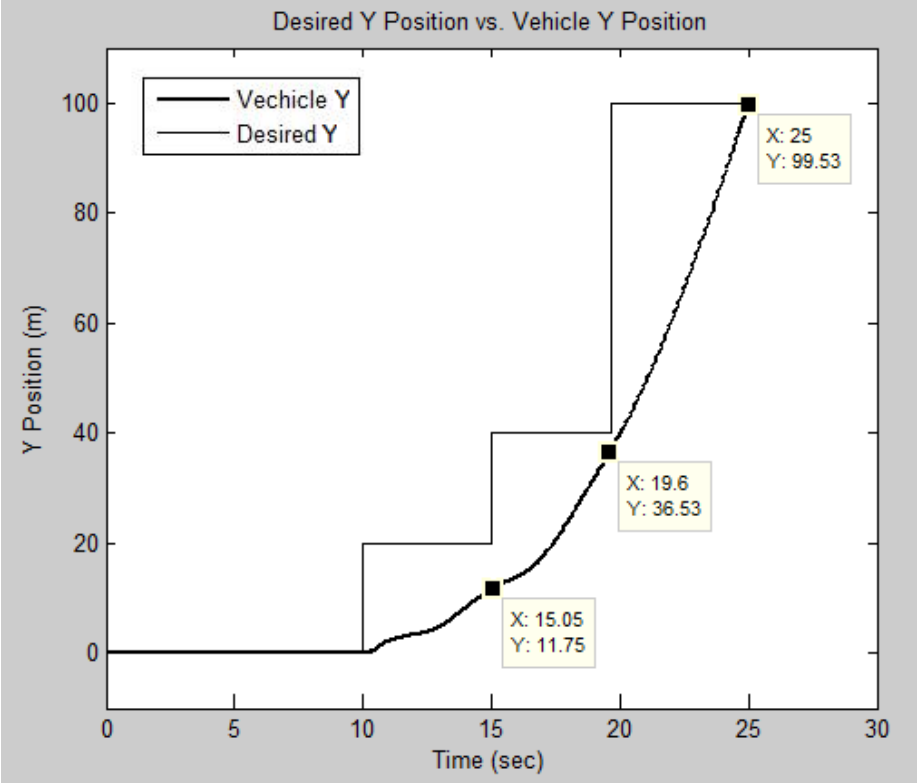

Figure 51 Desired Y Position vs. Actual Y Position of the Vehicle

CHAPTER 5

OPTIMAL CONTROL

An optimal controller is designed using the dynamical model of the vehicle. Two methods were tried for the controller design but only one managed to give a reasonable output. The first method was the Steepest Descent Algorithm (SDA) with Simultaneous Perturbation Stochastic Approximation (SPSA) method to approximate the gradient and the other is the Genetic Algorithm (GA).

With SDA algorithm the optimization process is started by creating an initial input sequence (i.e., the unknown sequence) for the system to begin. One iteration of the SDA is described as follows: After the input sequence is given, cost function is evaluated and the gradient calculation is done by the (SPSA) algorithm and an approximation to the gradient is obtained. Next, a line search is done along the negative gradient line by employing an exhaustive search technique and the next iteration point is found. This process is repeated successively until a local (maybe a global) minimum is found.

For the GA, the optimization process is initiated by creating a feasible initial population for the system to begin with. Next, the genetic search algorithm is executed via the MATLAB's GA toolbox. The genetic algorithm is used for a couple of hundred generations through a process which allows the fittest members to live and pass to the next generation and create new feasible members with the help of the elite members while eliminating unfeasible ones.

5.1 Cost Function and Boundary Conditions

For the optimization process a cost function is constructed for the SIMULINK model. The mathematical expression of the cost function is given below:

$$Cost_{t0-tf}(\bar{I}) = Cost\_Error_{t0-tf}(\bar{I}) + Cost\_Energy_{t0-tf}(\bar{I}) \tag{5.1}$$

where

$$Cost\_Error_{t0-tf}(\bar{I}) = \int_{t0}^{tf} (X(\bar{I}) - X_{desired})^2 + \int_{t0}^{tf} (Y(\bar{I}) - Y_{desired})^2 + \int_{t0}^{tf} (V_{x\_body}(\bar{I}) - V_{x\_body\,desired})^2 \tag{5.2}$$

$$Cost\_Energy_{t0-tf}(\bar{I}) = C_1 \int_{t0}^{tf} (EngineOutput(\bar{I}))^2 + C_2 \int_{t0}^{tf} (BrakeOutput(\bar{I}))^2 \tag{5.3}$$

After the cost is evaluated by the SIMULINK program, the information is passed to the MATLAB workspace and used by the optimization algorithms.

The boundary conditions are normalized in such a way that only an array can be inserted into the optimization algorithms and that every input must be between 0 and 90. The steering input is inserted into a function to convert the matching value to radians with the function below:

$$SteeringInput = F(x) = (x - 45)/225 \tag{5.4}$$

5.2 Steepest Descent Algorithm (SDA)

As the first method used for optimization process the SDA is given below:

$$X_{n+1} = X_n + \gamma_n \nabla F(X_n) \quad \text{while } n \geq 0 \tag{5.5}$$

The algorithm relies on the gradient of the present point and performs a line search along the negative gradient direction to determine the next iteration point. To perform a line search first the gradient information is required; however calculating the gradient analytically is very complicated or nearly impossible. It should be calculated numerically, i.e., approximately.

The SIMULINK model uses three inputs for every step size of the simulation in order to run the model. As an example, for a 50 second run with 0.01 second fixed step size one needs a matrix $\bar{I}$ of 3 rows and 5000 columns. Considerable time is required just to calculate the gradient of a cost function with the input matrix of such large element sizes. At this point SPSA is used to avoid the necessity of running a simulation for each element of the input matrix to get its partial derivative.

The specialty of the SPSA algorithm is that it needs two function evaluations independent from the dimension of the optimization problem. This enables the algorithm run much raster and allows a considerable decrease in the time duration of the optimization process per iteration.

The algorithm works with random perturbation of all elements of $\hat{\theta}_k$ together in order to obtain two function evaluations $f(\hat{\theta}_k + c_k\Delta_k)$ and $f(\hat{\theta}_k - c_k\Delta_k)$. Gradient estimation is done by subtracting these two terms and $\hat{g}_k(\hat{\theta}_k)$ is formed by dividing the difference with the individual components of the perturbation vector. For two-sided SP;

$$\hat{g}_k(\hat{\theta}_k) = \begin{bmatrix} \dfrac{f(\hat{\theta}_k + c_k\Delta_k) - f(\hat{\theta}_k - c_k\Delta_k)}{2c_k\Delta_{k1}} \\ \vdots \\ \dfrac{f(\hat{\theta}_k + c_k\Delta_k) - f(\hat{\theta}_k - c_k\Delta_k)}{2c_k\Delta_{kp}} \end{bmatrix}$$

$$= \frac{f(\hat{\theta}_k + c_k\Delta_k) - f(\hat{\theta}_k - c_k\Delta_k)}{2c_k} \left[\Delta_{k1}^{-1}, \Delta_{k2}^{-1}, \ldots, \Delta_{kp}^{-1}\right]^T \tag{5.2}$$

where $\Delta_k = \left[\Delta_{k1}, \Delta_{k2}, \ldots, \Delta_{kp}\right]^T$ is the distribution of the user-specified p-dimensional random perturbation vector. (Superscript "T" denotes vector transpose).

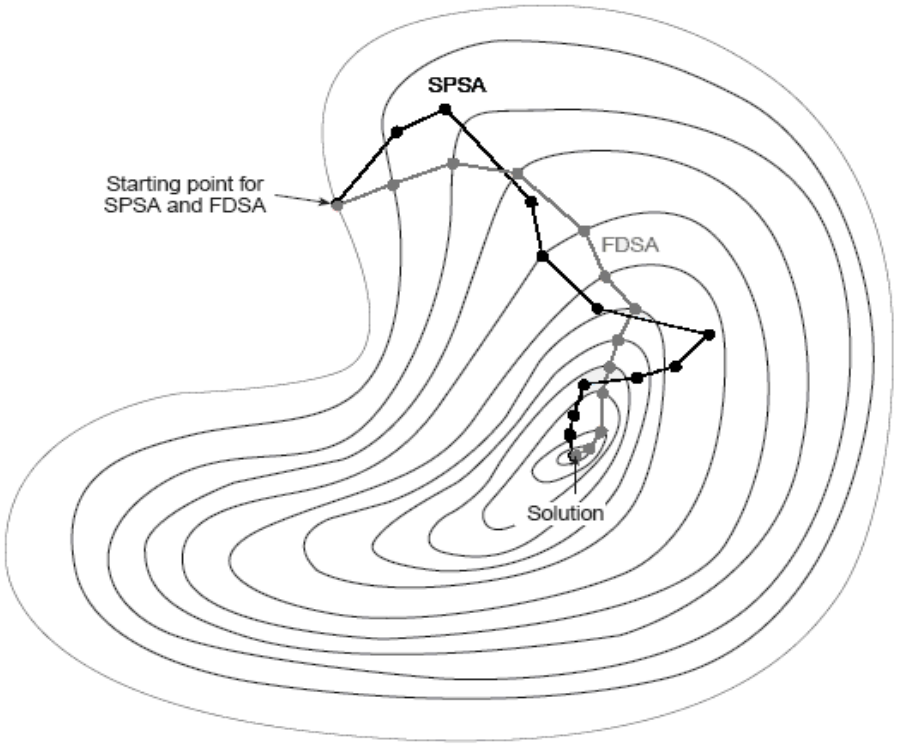

Figure 52 Relative Search Patterns for Two Dimensional a Problem for SPSA and FDSA Algorithms [30].

The number of function evaluations needed by the SPSA algorithm is only two measurements independent of individual component number since the numerator is same in all components of gradient.

5.2.1 Implementation of the SPSA

The SPSA algorithm works iteratively to produce an estimation sequence with six steps. The steps are given below [30]:

Step 1: Initialization and coefficient selection. Set counter index to $k=1$. Pick an initial guess and a set of non-negative coefficients $a, c, A, \alpha \text{ and } \gamma$ in the SPSA gain sequences $a_k = a/(A+k)^{\alpha}$ and $c_k = c/k^{\gamma}$. The choice of the gain sequences (a_k and c_k) is critical to the performance of SPSA (as with all stochastic optimization algorithms and the choice of their respective algorithm coefficients). Spall [30] provides some guidance on picking these coefficients in a practically effective manner. In cases where the elements of θ have very different magnitudes, it may be desirable to use a matrix scaling of the gain a_k if prior information is available on the relative magnitudes. The next section discusses a second-order version of SPSA that automatically scales for different magnitudes.

Step 2: Generation of the simultaneous perturbation vector. By a Monte Carlo process, a p-dimensional random perturbation vector Δ_k is generated, where each of the p components of Δ_k is independently generated from a zero mean probability distribution satisfying the preceding conditions. A simple (and theoretically valid) choice for each component of Δ_k is to use a Bernoulli ±1 distribution with probability of 1/2 for each ±1 outcome. Note that uniform and normal random variables are not allowed for the elements of Δ_k by the SPSA regularity conditions (since they have infinite inverse moments).

Step 3: Loss function evaluations. Obtain two measurements of the loss function $L(.)$ based on the simultaneous perturbation around the current $\hat{\theta}_k : y(\hat{\theta}_k + c_k\Delta_k)$ and $y(\hat{\theta}_k - c_k\Delta_k)$ with c_k and Δ_k coming from Steps 1 and 2.

Step 4: Gradient approximation. Generate the simultaneous perturbation approximation to the unknown gradient $g(\hat{\theta}_k)$ as follows:

$$\hat{g}_k(\hat{\theta}_k) = \frac{y(\hat{\theta}_k + c_k\Delta_k) - y(\hat{\theta}_k + c_k\Delta_k)}{2c_k} \begin{bmatrix} \Delta_{k1}^{-1} \\ \Delta_{k2}^{-1} \\ \vdots \\ \Delta_{kp}^{-1} \end{bmatrix} \quad [3.5]$$

where Δ_{ki} is the ith component of the Δ_k vector (which may be ±1 random variables as discussed in Step 2); note that the common numerator in all p components of $\hat{g}_k\left(\hat{\theta}_k\right)$ reflects the simultaneous perturbation of all components in $\hat{\theta}_k$ in contrast to the component-by-component perturbations in the standard finite-difference approximation.

Step 5: Updating u estimate. Use the standard SA form

$$\hat{\theta}_{k+1} = \hat{\theta}_k - a_k\hat{g}_k(\hat{\theta}_k) \quad [3.6]$$

to update $\hat{\theta}_k$ to a new value $\hat{\theta}_{k+1}$. Modifications to the basic updating step in Equation [3.6] are sometimes desirable to enhance convergence and to impose constraints. These modifications prevent or alter the update to the new value of θ if the "basic" value from Equation [3.6] appears undesirable.

Step 6: Iteration or termination. Return to Step 2 with k+1 replacing k. Terminate the algorithm if there is little change in several successive iterates or the maximum allowable number of iterations has been reached.

During this study line search is done with a different algorithm then the above algorithm suggests. So $a_k = a/(A+k)^{\alpha}$ part was not used.

5.2.2 Exhaustive Line Search

After an approximate gradient is obtained via the SPSA algorithm, it can be used for a line search to find the minimum point in the negative direction of the

gradient. The method to perform the line search is the Exhaustive Line Search since it is much easier to apply and can give the profile of the cost function along the gradient.

The method is slicing the gradient line up to a decided maximum number of points with equal step sizes and then performing a cost evaluation at each step to make a comparison to find the point which has the minimum cost value (Figure 53) [29].

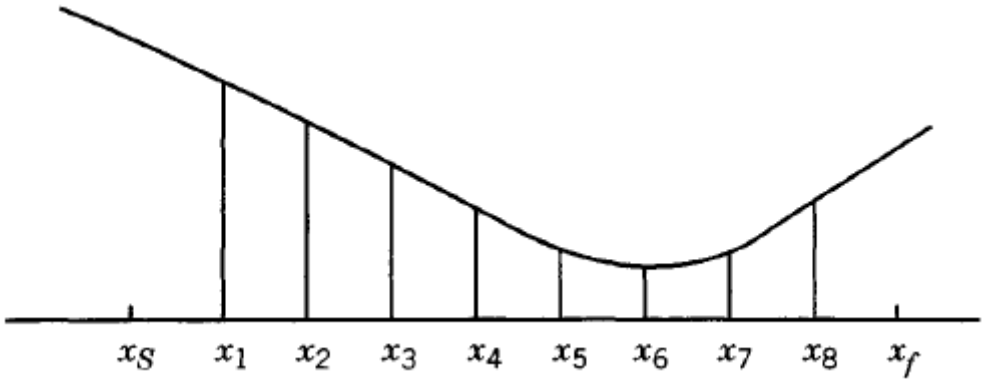

Figure 53 Demonstration of Exhaustive Nine Step Search []29]

5.2.3 Results of the SDA

The minimum cost value obtained with the SDA is 11249. This cost value is obtained after 52 iterations of SDA with 100 steps of exhaustive search. The corresponding X-Y plot and Vx body plots with respect to the desired ones are given below:

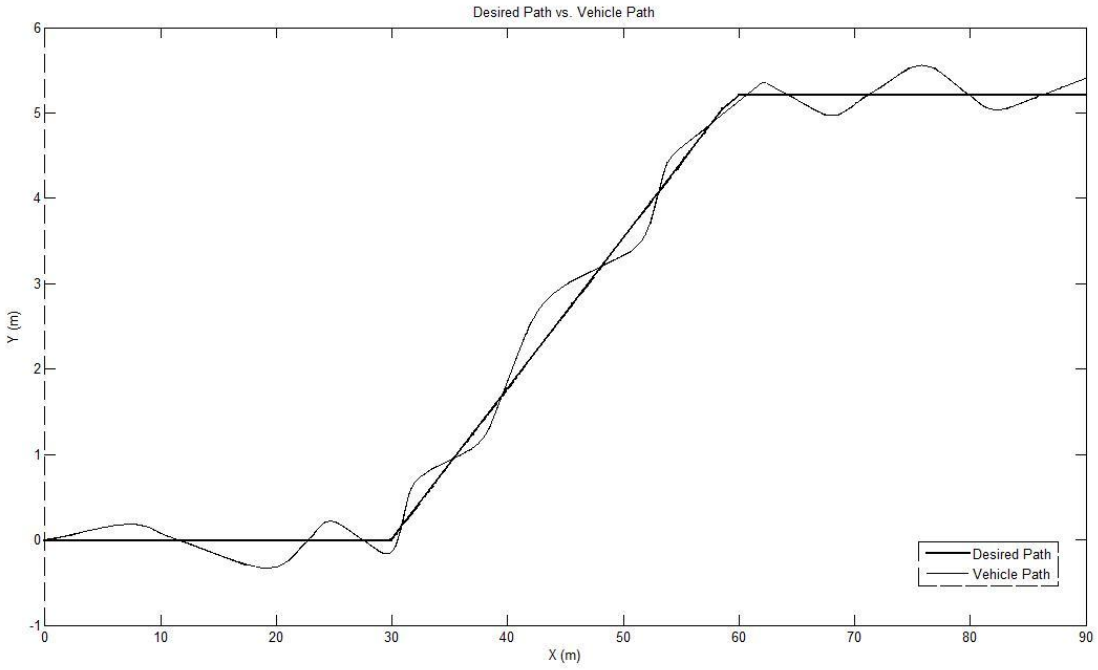

Figure 54 Vehicle's X-Y position vs. Desired X-Y Position at Cost Value 11249

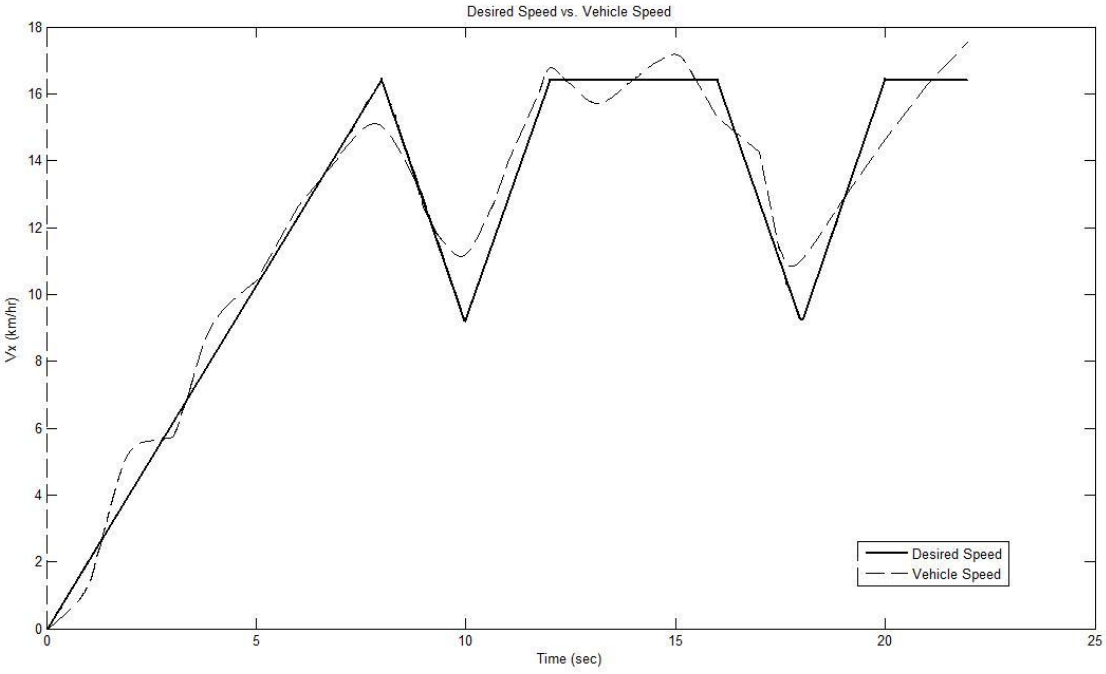

Figure 55 Vehicle's Vx vs. Desired Vx at Cost Value 11249

5.3 Genetic Search Algorithm (GA)

The input for the GA optimization process is the same as the SDA optimization, but it has to be slightly modified to be used by GA optimization toolbox of MATLAB. The GA can only take a vector as an input for the optimization process so the matrix is converted to a vector as shown below (Figure 56):

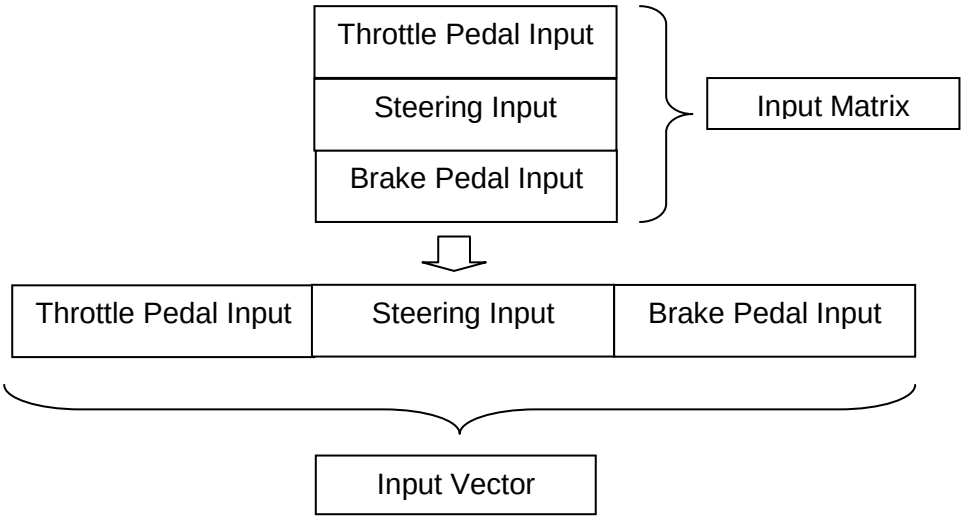

Figure 56 Transformation of Input Matrix to Input Vector

After generating suitable inputs for the GA toolbox, the next step is executing it by GA optimization toolbox of MATLAB.

5.3.1 Implementation of GA

The GA algorithm works iteratively to produce a population with a given rule set. The rule set is given by Optimal Tool. The importance of the rule set is that the performance of GA is largely based on it as the basic parameters are introduced with it. The rule set of the GA is given below:

Table 5 Rule Set Used for GA Execution

Option Name		Input
Population	Population Type	Double Vector
	Population Size	350
	Create Function	Feasible Population
	Initial Range	[0;90]
Fitness Scaling		Rank
Selection		Stochastic Uniform
Reproduction	Elite Count	10
	Crossover Function	0.75
Mutation	Mutation Function	Uniform
	Rate	0.5
Crossover	Crossover Function	Scattered
Migration	Direction	Forward
	Fraction	0.4
	Interval	15
Algortihm Settings	Initial Penalty	15
Stopping Criteria	Generations	600
	Stall Generation	15

5.4 Results of the Optimization Process

Running the GA with the given rule set (
Table 5) for 350 iterations minimized the cost function to 8542. As the fitness value of the best individual did not get any better than 8542, after 543 iterations, the algorithm stopped and resulting individual was sent to MATLAB workspace.

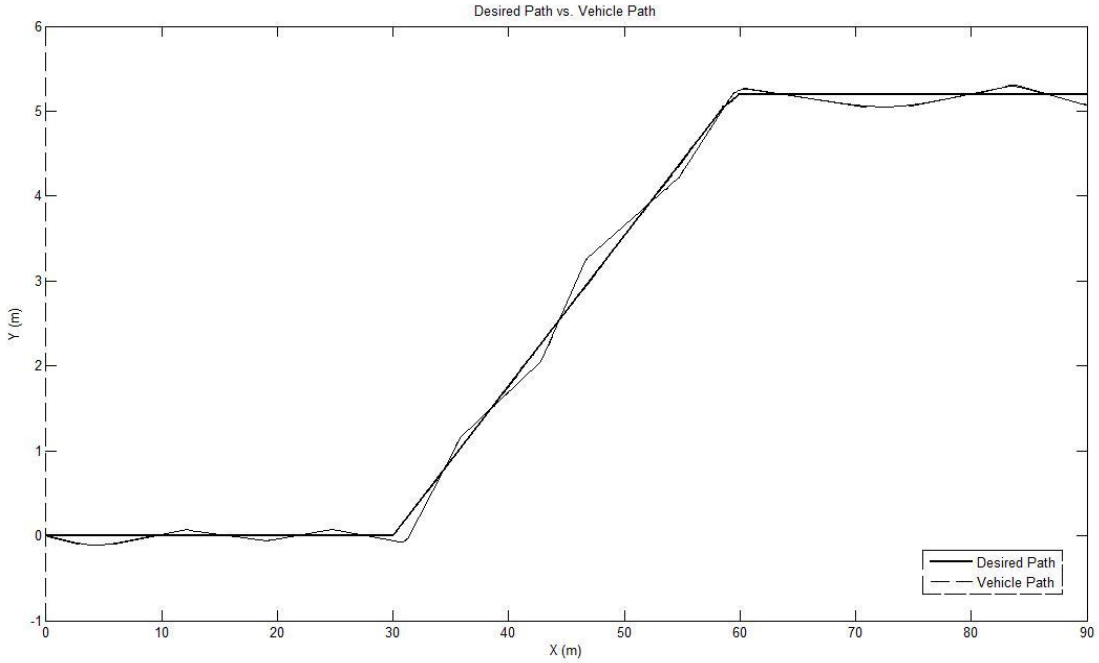

Figure 57 Desired and Actual Paths at Cost Value 8542

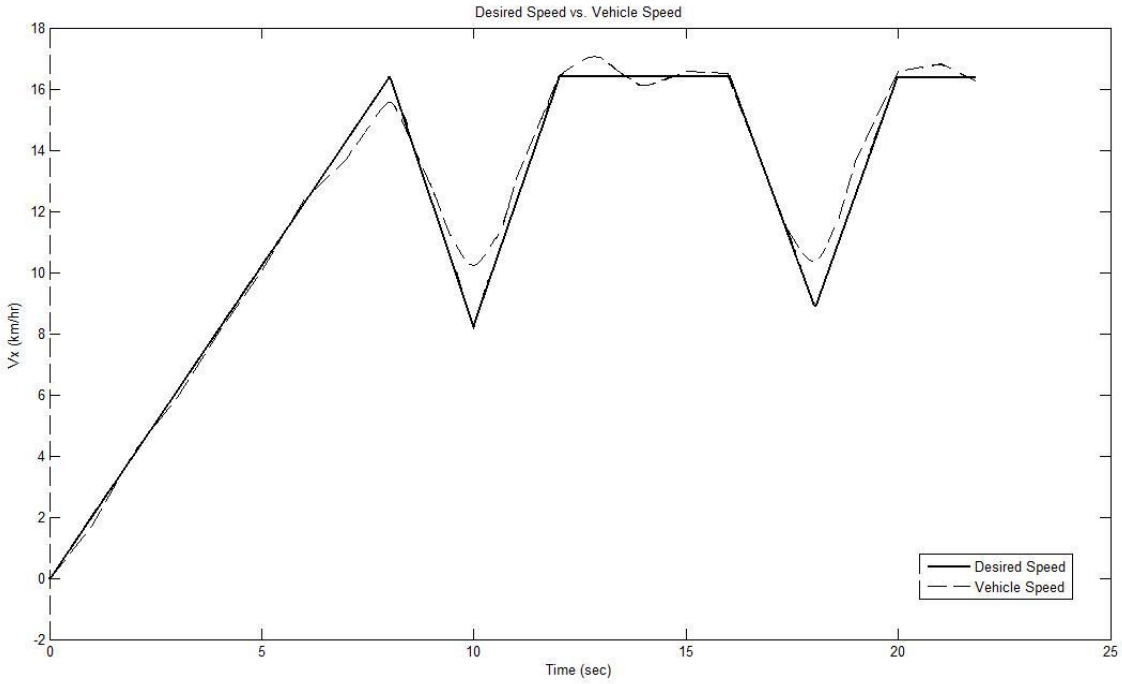

Figure 58 Desired and Actual Vehicle Speeds at Cost Value 8542

CHAPTER 6

CONCLUSION

In this study, a dynamical 6DoF four wheeled vehicle model is constructed. After introducing the model its validity is verified via simulation runs and an optimal controller for the model is designed.

The 6DoF model is constructed after modeling the subsystems of a car, namely internal combustion engine, transmission, tires, suspension, brakes, air drag and slip. The models of these components are required in order to determine the forces that the vehicle is subjected to.

A navigation block with PID controllers is designed to verify the model. With the designed navigation block, some simulation studies were performed and model responses to simulation inputs are observed to be consistent.

Completion of the verification process was followed by designing two optimal controllers for the system by employing the SDA and GA optimization techniques. The results of the GA are better than the SDA; however total iteration numbers suggest that the SDA as a better alternative. The results could be improved with better cost function definition by tuning the energy cost coefficients and different line search methods for the SDA, or different rule sets for the GA.

As a future work, a more comprehensive model could be built by improving force generating blocks such as employing quarter car model for the suspension, adding longitudinal slip, and/or advanced brake models. Also, as regards the simulations, instead of a planar surface an inclined or parabolic surface can be employed added with road noise such as humps or holes. Also different type of engine models and controller types can be implemented on the model to see their effects for the system. The simulation should be optimized to decrease the simulation time and parallel computing should be employed also to perform simulations faster.

REFERENCES

[1] Andrezejewkski R., Awrejcewics J., A. F., “Nonlinear Dynamics of a Wheeled Vehicle”, Springer, 2005.

[2] Tran, T.H., “Modelling and Control of Unmanned Ground Vehicles”, Ph.D. Thesis, University of Technology, Sydney, Australia, 2007.

[3] Malhotra, S., “Simulation of Streering Systems for Robotic Vehicles”, Master’s Thesis, FSU, 2006.

[4] Rajamani R., “Vehicle Dynamics and Control”, Springer, 2006.

[5] Reza N. J., “Vehicle Dynamics: Theory and Applications”, Springer, 2008.

[6] “Euler Angles”, Wikipedia, the Free Encyclopedia. 20 Jan 2009, 18:09 UTC. Wikimedia Foundation, Inc., 29 Feb 2009, <http://en.wikipedia.org/wiki/Euler_angles>.

[7] “Understanding D.C. Motor Characteristics”, MIT, Mech. Eng., 29 Jan 2009, <http://lancet.mit.edu/motors/motors3.html>.

[8] “Simulink - Vehicle Acceleration – 7”, David Grieve. 04 Nov 2005. MIT, 10 Feb 2009, <http://lancet.mit.edu/motors/motors3.html>.

[9] Kiencke U., Nielsen L., “Automotive Control Systems for Engine, Driveline, and Vehicle”, Springer, 2005.

[10] “ME 452 Automotive Vehicle Dynamics Course Notes”, PSU, Mech. Eng., Sean Brennan 2004, <http://www.mne.psu.edu/brennan/ME452>.

[11] Dorf C. Richard, Bishop H. Robert, “Modern Control Systems“, Prentice Hall, 2001.

[12] “Rolling Resistance”, Wikipedia, the Free Encyclopedia, 3 Apr 2009, 16:03 UTC. Wikimedia Foundation, Inc., 12 May 2009, <http://en.wikipedia.org/wiki/Rolling_resistance>.

[13] “Friction”, Wikipedia, the Free Encyclopedia, 13 Apr 2009, 22:52 UTC. Wikimedia Foundation, Inc., 12 May 2009, <http://en.wikipedia.org/wiki/Friction>.

[14] Jang B., Karnopp D., “Simulation of Vehicle and Power Steering Dynamics Using Tire Model Parameters Matched to Whole Vehicle Experimental Results”, Vehicle System Dynamics, vol. 33, no. 2, pp. 121-133, 2000.

[15] MATLAB Help, automotive suspension, Mathworks, 2006.

[16] “Brake Hydraulic Theory”, Wordpress, Mechanical Daydream, 17 Apr 2009, <http://enderw88.wordpress.com/automotive-theory/brake-system-theory/>.

[17] “aerodynamics.gif”, Pressroom, 21 Apr 2009, 14:42 UTC. Wikipedia Foundation, Inc., 01 May 2009, <http://www.pressroom.com.au/pressroom/sample/presskits/99celicaspecs/aerodynamics.gif>.

[18] Giancoli D. C., “Physics for Scientists and Engineers with Modern Physics”, Prentice Hall, 1999.

[19] Stone M. R., Demetriou M. A., “Modeling and Simulation of Vehicle Ride and Handling Performance”, IEEE Int. Symp. on Intelligent Control (ISIC 2000) MB-5, pp. 85-87

34[20] Shim T., Ghike C., “Understanding the Limitations of Different Vehicle Models for Roll Dynamics Studies”, Vehicle System Dynamics., vol. 45, no. 3, pp. 191-216, March 2007.

[21] Ogata K., “Modern Control Engineering”, Prentice Hall, 1997.

[22] “Building Intelligent Robots”, Cs Brown Edu., 08 Mar 2002, 18 May 2009, <http://www.cs.brown.edu/~tld/courses/cs148/02/images/pid.gif>.

[23] Kirk D. E., “Optimal Control Theory: An Introduction”, Dover Pub., 2004.

[24] Osborn R. P., “Independent Control of All-Wheel-Drive Torque Distribution”, Vehicle System Dynamics, vol. 44, no. 7, pp. 529-546, June 2006.

[25] Braghin F., Cheli F., Corradi R., Tomasini G., Sabibioni E., “Active Anti-Rollover System For Heavy-Duty Road Vehicles”, Vehicle System Dynamics., vol. 46, no. 1, pp. 653-668, Jan. 2008.

[26] Daofei L., Shangquian D., Fan Y., “Integrated Vehicle Chassis Control Based on Direct Yaw Moment’ Active Steering and Active Stabilizer”, Vehicle System Dynamics, vol. 46, no. 1, pp. 341-351, Jan. 2008.

[28] Rajamani R., “Vehicle Dynamics and Control”, Springer, 2006.

[29] Singiresu S. R., “Engineering Optimization: Theory & Practice”, Wiley, 1996.

[30] James C. Spall, “An Overview of the Simultaneous Perturbation Method for Efficient Optimization”, Johns Hopkins APL Technical Digest, vol 19, no 4, 1998.